



저작자표시-비영리-변경금지 2.0 대한민국

이용자는 아래의 조건을 따르는 경우에 한하여 자유롭게

- 이 저작물을 복제, 배포, 전송, 전시, 공연 및 방송할 수 있습니다.

다음과 같은 조건을 따라야 합니다:



저작자표시. 귀하는 원저작자를 표시하여야 합니다.



비영리. 귀하는 이 저작물을 영리 목적으로 이용할 수 없습니다.



변경금지. 귀하는 이 저작물을 개작, 변형 또는 가공할 수 없습니다.

- 귀하는, 이 저작물의 재이용이나 배포의 경우, 이 저작물에 적용된 이용허락조건을 명확하게 나타내어야 합니다.
- 저작권자로부터 별도의 허가를 받으면 이러한 조건들은 적용되지 않습니다.

저작권법에 따른 이용자의 권리는 위의 내용에 의하여 영향을 받지 않습니다.

이것은 [이용허락규약\(Legal Code\)](#)을 이해하기 쉽게 요약한 것입니다.

[Disclaimer](#)

치의과학석사 학위논문

Study of synthetic peptide
conjugated hydrogel on
bone regeneration

골재생효과에 대한 합성 펩타이드
함유 하이드로젤의 기능성 연구

2016년 2월

서울대학교 대학원
치의과학과 치의재생생명공학전공
조 범 수

Abstract

Study of synthetic peptide conjugated hydrogel on bone regeneration

Beom Soo Jo

Dental Regenerative Biotechnology Major
Graduate school, Seoul National University
(Supervised by Professor Yoon Jeong Park)

Stem cell carrying biomaterials including porous scaffolds, membranes have gained some success in bone regeneration. Among them, injectable hydrogel systems have received much attention due to their versatile and tunable characteristics and ease of application in the defect without the need of surgery. In addition, bioactive agent including protein, peptide and genetic materials also can be loaded into the hydrogel and the controlled

release of these agent can favor the bone regenerative potential. Despite the efficacy of these bioactive molecules, however, the effective loading into the gel has been limited to the physical mixing. The simple mixture of bioactive agent and hydrogel have limited release control, due to burst release, therefore the alternative conjugating method of molecules and hydrogel is required.

The chemical conjugation of protein with hydrogel might alter the efficacy of the protein, therefore it was anticipated that the synthetic peptide with functional moiety with chemical conjugation would be an alternate for the hydrogel conjugation. Herein, synthetic peptide from osteopontin termed as collagen binding motif (CBM) was attempted as it has defined osteogenic activity from the previous studies. The CBM peptide (CBMP) has osteogenic differentiation capacity to mesenchymal stem cells and thus been chosen in combination with hydrogel. The hydrogel has tyrosine functional group, and was designed to chemically conjugating with matching tyrosine group under the triggering by hydrogen peroxide with horseradish peroxidase (HRP). The CBMP possesses tyrosine functional group, therefore hydrogel crosslinking was attempted with CBMP under the H_2O_2 /HRP condition even containing stem cells.

The CBMP-crosslinked hydrogel demonstrated well survival of incorporating stem cells. The CBMP-crosslinked hydrogel increased osteogenic differentiation of cultured stem cells, as reflected by the increased osteogenic marker protein expression, calcein acetoxymethyl ester (calcein AM) staining, alkaline phosphatase activity staining, mineral deposition measured by Energy Dispersive Spectrometer (EDS). The further *in vivo*

study confirmed the stem cells in the CBMP-crosslinked hydrogel significantly improved bone formation capacity in the rat calvarial defect as similar extent to that of BMP-containing hydrogel. Taken together, the CBMP conjugating hydrogel was demonstrated to have increased potential for osteogenic differentiation of stem cells, and moreover can be suggested as a tool as bioactive delivery vehicle of stem cells in tissue regenerative practice.

Keywords : Bone regeneration, Synthetic peptide, Collagen binding motif, hydrogel, stem cell

Student Number : 2013-23551

Contents

Abstract	i
List of Figure	vi
List of Table	viii
I. Introduction	2
II. Materials and methods	5
2.1. Materials	5
2.2. Synthetic peptide and its osteogenic activity assay	6
2.2.1 Peptide synthesis and purification	6
2.2.2 Cell culture	7
2.2.3. Osteogenic differentiation by CBMP : Western blot assay	7
2.2.4. Osteogenic differentiation by CBMP : Alkaline phosphatase activity assay	8
2.2.5. Osteogenic differentiation by the CBMP : Alizarin red S stain assay	9
2.3. Synthetic peptide–hydrogel and its osteogenic activity	10
2.3.1. Preparation of peptide cross–linked hydrogel	10
2.3.2. Incorporation efficiency of biomolecule in hydrogel	11
2.3.3. Preparation of 3D cell culture	12
2.3.4. Cell proliferation in the peptide–hydrogel	12
2.3.5. Osteogenic potential of hPDLSCs cultured in peptide–hydrogel : Immunofluorescence assay	13
2.3.6. Osteogenic differentiation of hPDLSCs in the peptide hydrogel : Quantitative real time polymerase chain reaction	

assay	14
2.3.7. Osteogenic differentiation of hPDLSCs in the peptide-hydrogel : mineral detection by energy dispersive spectrometer assay	15
2.3.8. In vivo osteogenic activity of hPDLSCs in peptide-hydrogel	16
2.3.8.1 Surgical procedure of application of hPDLSCs peptide-hydrogel in the rat calvarial defect model	16
2.3.8.2 In vivo osteogenesis measured by micro-computed tomography analysis	17
2.3.8.3 Histological analysis of osteogenesis by hPDLSCs in the peptide-hydrogel applied in the calvarial defect	17
2.4. Data analysis	18
III. Results	22
3.1. CBMP synthesis and its osteogenic activity	22
3.2. Peptide conjugated hydrogel	28
3.2.1. Incorporation efficiency of peptide in the hydrogel	28
3.2.2. Evaluation of cell proliferation in a 3D environment	31
3.2.3. Peptide-conjugated hydrogel for osteogenic ability	35
3.2.4. New bone formation by the hPDLSCs in the peptide-hydrogel	42
IV. Discussion & Conclusion	48
V. Reference	54
Abstract in Korean	62

List of Figures

Figure 1. Surgical procedure	19
Figure 2. LC/MS results for collagen binding motif peptide and the control peptide after purification.	24
Figure 3. Expression of osteogenic markers	25
Figure 4. Effect of ALP expression by CBMP	26
Figure 5. Effect of calcium deposition by CBMP	27
Figure 6. Efficiency of biomolecule conjugation with hydrogel ·	29
Figure 7. Image of cultured cell in biomolecule conjugated hydrogel	32
Figure 8. Proliferation assay of biomolecule conjugated hydrogel by CCK-8	33
Figure 9. Proliferation assay of biomolecule conjugated hydrogel by DNA contents assay	34
Figure 10. Fluorescence images of expression of osteogenic marker as biomolecule conjugation with hydrogel	37

Figure 11. Quantification of fluorescence intensities of Runx2 and OCN	38
Figure 12. Expression of osteogenic markers as biomolecule conjugation with hydrogel	39
Figure 13. Image of calcium deposition and EDS analysis	40
Figure 14. 3D micro-CT images	44
Figure 15. Bone regeneration area and bone mineral density evaluated by micro computed tomography examination	45
Figure 16. H&E staining	46
Figure 17. Masson's trichrome stain	47
Figure 18. Schematic depicting the overall experimental model ·	53

List of Tables

Table 1. The nucleotide sequences of the primers used for constructing the plasmids and osteogenic markers	20
Table 2. Groups of the animal experiment of new bone formation	21
Table 3. Groups of incorporation efficiency experiment for biomolecule-hydrogel	30
Table 4. Surface elemental analysis of hydrogels by EDS	41

Study of synthetic peptide
conjugated hydrogel on
bone regeneration

Beom Soo Jo

Dental Regenerative Biotechnology Major
Graduate school
Seoul National University

(Supervised by Professor Yoon Jeong Park)

I . Introduction

Biomaterial based scaffolds such as porous collagen matrices, synthetic polymeric porous blocks, injectable polymeric hydrogels have gained some successes in bone regeneration application [1, 2]. As these biomaterials have proved biocompatibility, the matrices have been used as tool for stem cell engineering purpose. In addition, the polymeric characteristic of the matrices enables incorporation of bioactive molecules including protein and peptide drug, thereby regulates the release kinetics from the matrices [3]. The controlled release of these protein and peptide drugs has been reported to significantly enhance the tissue regeneration capacity. Among the matrices, injectable hydrogel has been attempted in this study. Injectable hydrogel has advantages over the other types of solid matrices, such as ease of application to the defect without the needs of surgical procedure, in situ formation of hydrogels has received much attention because of the ease of application using minimally invasive techniques for tissue regenerative medicine and drug delivery systems [4]. Although the significant osteogenic potential of growth factor such as bone morphogenetic protein (BMP), platelet derived growth factor (PDGF) have been proved, the clinical application has been limited due to possible immunogenicity, alteration of physical property during the incorporation procedure and complication related concerns [5, 6]. As an alternative to the growth factor and protein, the synthetic peptide can be proposed as the peptide has sufficient stability, less immunogenicity, ease of handling when conjugating with biomaterials [7–9]. As the bioactive agent with the hydrogel, the

synthetic peptide derived from osteopontin has been attempted in this study.

Herein, the synthetic peptide termed as collagen binding motif (CBM) has been applied to conjugation with hydrogel. The CBM peptide (CBMP) has the same sequence to that of 135 - 147 amino acid sequence in osteopontin. The CBM in osteopontin has been defined to specifically bind to collagen, and induce the mineralization in simulated body fluid [10–11]. In addition, the CBMP specifically directed the osteogenic differentiation of mesenchymal stem cells, while arrested adipogenic differentiation [10, 12]. To this regard, combination with the CBMP with hydrogel was anticipated to improve bone formation of stem cells in the defect. The loading method of bioactive agent in the hydrogel determines the final tissue regenerative outcomes, as the incorporated agent has to be localized in the applied site [13]. Simple physical mixture of bioactive agent and hydrogel has been attempted, however, the loading efficiency is relatively low and the burst release of the agent from the hydrogel remains to be improved [14]. The chemical conjugation is therefore favored the localization of the active agent, however the protein conjugation might alter the stability of protein while incorporation procedure [15]. In contrast to protein, the synthetic peptide can be further modified to contain functional chemical group, which favors the crosslinking without the concern of alteration of stability. The hydrogel in this study is from gelatin, and forms firm gels under the hydrogen peroxide / horseradish peroxidase (HRP) by creation of tyrosine–tyrosine conjugation. This tyrosine–tyrosine conjugation is even advantageous over the other crosslinking agent for amide bond

creation, as it does not have harmful effect on the incorporating cells. The CBMP was designed to contain tyrosine residue, therefore the incorporation in the hydrogel was attempted by in situ conjugation using hydrogen peroxide and HRP, in presence of stem cells. The stem cells in this study was human periodontal ligament stem cells (hPDLSCs), derived from periodontal ligament. The hPDLSCs has been known to exhibit similar mesenchymal stem cell characteristics to that of bone marrow stem cells (BMSCs), and advantages including obtaining procedure is not much invasive than BMSCs [16].

Herein, the osteogenic potential of hPDLSCs by the CBMP, in-situ hydrogel conjugation of CBMP, the characterization and osteogenic potential of CBMP conjugated hydrogel *in vitro* and *in vivo* will be detailed discussed.

II. Materials and methods

2.1 Materials

Rink amide resin (mM/g) with Fmoc-amino acids was purchased from Beadtech (Seoul, Korea). 2-(1H-benzotriazol-1-yl)-1,1,3,3-tetramethyluronium hexafluorophosphate (HBTU) was purchased from Advanced ChemTech (Louisville, KY, USA). Piperidine, diisopropylethylamine (DIPEA), triisopropylsilane (TIS), phenol, and thioanisole were obtained from Sigma-Aldrich. Tetrahydrofuran (THF) acetonitrile and trifluoroacetic acid (TFA) were purchased from Burdick & Jackson (Morris Plains, NJ, USA). 1,2-ethanedithiol (EDT) was purchased from Sigma-Aldrich (MO, USA). Anti-Runt-related transcription factor 2 (Runx2), anti-osteocalcin (OCN), and anti-OPN were purchased from Abcam (Cambridge, UK). anti-Smad1/5/8, anti-pSmad1/5/8, and anti-collagen type I were purchased from Santa Cruz Biotechnology, Inc. (Dallas, TX, USA), and anti-glyceraldehyde 3-phosphate dehydrogenase (GAPDH) was purchased from Merck Millipore (Darmstadt, German). Bone morphogenic protein (BMP)-2 was purchased from R&D Systems (Abingdon, UK). All other reagents and products were purchased from Sigma-Aldrich (St. Louis, MO, USA) unless noted otherwise.

2.2 Synthetic peptide and its osteogenic activity assay

2.2.1 Peptide synthesis and purification

The CBMP and control peptide (CP) exhibiting tyrosine were synthesized using Fmoc chemistry by solid phase peptide synthesis according to the literature [17]. Deprotection and cleavage were achieved by the treatment with a mixture of TFA/water/thioanisole/ethanedithiol (8.5/0.5/0.5/0.5, v/v/v/v) or TFA/TIS/water (95/2.5/2.5, v/v/v) at room temperature for 3-4 hours. A 2-chlorotrityl chloride resin was pre-swollen in N,N-dimethyl formamide (DMF) and the Fmoc-protecting groups of the resin and amino acids were removed using 30 % piperidine in DMF, 10 eq. DIPEA, 5 eq. HBTU, and 5 eq. of Fmoc-protected amino acid, calculated according to the loading of the resin. The peptide-resin was dried using methylene chloride. The peptide cleavage solutions were mixed with diethyl ether, and the aqueous peptide solutions were lyophilized. The prepared peptides were purified by reversed-phase high-performance liquid chromatography (Waters AutoPrep system, MA, Milford, USA) using a Vydac C18 column (Grace, Columbia, MD, USA) and a gradient of water/acetonitrile containing 0.1 % TFA. The peptides were characterized in terms of molecular weight by LC/MS and were found to have the expected molecular weight (CBMP : 2262, CP : 2227). Peptide purity was above 98 %.

2.2.2 Cell culture

The hPDLSCs used in this study were from Dr. Gene Lee, Seoul National University, Korea. The cells were cultured in Minimum Essential Medium Eagle Alpha Modifications (α -MEM) (Hyclone, Road Logan, UT, USA) supplemented with 10 % fetal bovine serum (FBS) and 1 % antibiotic-antimycotic solution (Thermo Fisher Scientific, Waltham, MA, USA). The hPDLSCs were cultured at 37°C under a humidified 95 % : 5 % (v/v) mixture of air and CO₂. Culture media was changed three times a week. For sub-culture upon reaching 80-90 % confluency, the cells were detached from culture flasks using a solution of 0.05 % Trypsin-0.02 % ethylenediaminetetraacetic acid (EDTA) and were then seeded onto fresh culture flasks at a ratio of 1:6.

2.2.3 Osteogenic differentiation by CBMP : Western blot assay

The hPDLSCs were incubated with phosphate buffered saline (PBS), CBMP (100 μ M), CP (100 μ M), or BMP-2 (100 ng/ml) for indicative times. At the end of the culture period, cells were lysed for 30 min at room temperature in lysis buffer (M-PER™ Mammalian Protein Extraction Reagent, Thermo Fisher Scientific, Waltham, MA, USA) containing protease inhibitor cocktail (Roche, Penzberg, Germany) and phosphatase inhibitor cocktail 2 (Sigma-Aldrich, St. Louis, MO, USA). Protein concentration was

measured with a bicinchoninic acid (BCA) assay kit (Thermo Fisher Scientific, Waltham, MA, USA). Equal aliquots of protein (40 μ g) were boiled for 7 min in 5x sample buffer (250 mM Tris-HCl (pH 6.8), 50 % glycerol, 10 % Sodium dodecyl sulfate (SDS), 500 μ M Dithiothreitol (DTT), 0.5 % bromophenol blue) and separated on 10 % SDS-polyacrylamide gel electrophoresis (PAGE) gels. Proteins were transferred to nitrocellulose membranes, washed with 1x TBS-T (20 mM Tris-HCl pH 7.6, 137 mM NaCl, containing 0.1 % Tween 20), and blocked for 1 hour at room temperature in 1x TBS-T with 5 % skim milk. The membranes were washed three times and incubated with primary antibodies (anti-Runx2 , anti-Smad1/5/8, anti-pSmad1/5/8, anti-collagen type I, anti-OCN, anti-OPN, anti-GAPDH (1:1000)) in TBS-T containing 5 % skim milk for 16 hours at 4°C. After three washes, the membranes were incubated with secondary antibodies (HRP-conjugated goat anti-rabbit IgG and HRP-conjugated goat anti-mouse IgG 1:2000 in TBS-T) for 1 hour, followed by another three washes. Protein bands were visualized with chemiluminescence reagent (Super Signal West Pico Chemiluminescent Substrate, Thermo Fisher Scientific, Waltham, MA, USA)

2.2.4 Osteogenic differentiation by CBMP : Alkaline phosphatase activity assay

For the determination of alkaline phosphatase (ALP) activity, hPDLSCs were grown to confluence in 24-well culture plates

and incubated with PBS, CBMP (100 μ M), CP (100 μ M), or BMP-2 (100 ng/ml) for 7 days in growth medium (GM, α -MEM supplemented with 10 % FBS and 1 % antibiotic-antimycotic solution) and osteogenic medium (OM, hMSC Osteogenic BulletKit, Lonza, Basel, Switzerland). The media was freshly changed every 3day with or without CBMP, CP, and BMP-2. For ALP staining, cells were washed three times with cold Dulbecco' s phosphate buffered saline (DPBS) and fixed 10 % NBF solution for 10 minute at room temperature. After additional washing with DPBS, they were stained using the ALP detection kit (Sigma-Aldrich, St. Louis, MO, USA) for 15 minute at room temperature, followed by two washes with water and air drying. Matrix mineralization was quantified by extracting the ALP stain with dimethyl sulfoxide (DMSO, Sigma-Aldrich, St. Louis, MO, USA) at room temperature for 10 minute. Absorbance of the extracted ALP stain was measured at 550nm.

2.2.5 Osteogenic differentiation by the CBMP : Alizarin red S stain assay

Matrix mineralization was determined by alizarin Red S. hPDLSCs were grown until confluent in 24-well culture plates and were then incubated with PBS, CBMP (100 μ M), CP (100 μ M), or BMP-2 (100 ng/ml) for 14 days in GM and OM. The media was freshly changed every 3 day with or without CBMP, CP, and BMP-2. For detection of calcium deposits, cells were washed three times with DPBS and fixed in 95 % ethanol for 15

min at room temperature. After an additional wash in water, the cells were incubated with 2 % alizarin red S (Sigma–Aldrich, St. Louis, MO, USA) in water for 20 min at room temperature, washed twice with water and then air drying. Matrix mineralization was quantified by extracting the alizarin red S stain with 10 % cetylpyridinium chloride (Sigma–Aldrich, St. Louis, MO, USA) at room temperature for 2 hours. Absorbance of the extracted alizarin red S stain was measured at 570nm.

2.3 Synthetic peptide–hydrogel and its osteogenic activity

2.3.1 Preparation of peptide cross–linked hydrogel

The gelatin–based hydrogel came from Dr. Ki–Dong Park, Ajou University of Korea. In situ peptide or protein conjugated hydrogels were prepared by simply mixing aqueous peptide and polymer solution in the presence of HRP (Sigma–Aldrich, St. Louis, MO, USA) and hydrogen peroxide solution (Sigma–Aldrich, St. Louis, MO, USA). HRP and hydrogen peroxide solutions were filtered for sterilization using a syringe filter with a pore size of 0.2 μ m. The peptide or protein conjugated hydrogels were prepared in 1 mL vials at room temperature. 200 μ l of the hydrogel polymer solution (5.5 wt %) including peptide (2 mM) or protein (20 ng/ml), dissolved in HRP solution (0.001 wt %) (solution A) and the same volume of

hydrogel polymer solution (5.5 wt %) dissolved in hydrogen peroxide solution (0.03 wt %) (solution B), was simply mixed and gently shaken. Finally, the same volumes of solutions A and B were mixed to obtain in situ peptide conjugated hydrogels. All solutions used were dissolved in DPBS.

2.3.2 Incorporation efficiency of biomolecule in hydrogel.

The amount of conjugated peptide in the hydrogels was quantified by relative fluorescence unit (RFU) intensity using fluorescein isothiocyanate (FITC)–peptides. FITC–peptide–hydrogels were prepared as previously described with different concentrations of peptide (0, 1, 10, 100 and 1000 μg). They were then washed to remove unconjugated peptides for 3 hours. The hydrogel samples were imaged using an LAS-1000 CCD camera (Fujifilm, Tokyo, Japan), and the RFU intensities were determined using a standard curve that was obtained from known concentrations and fluorescence intensities of the FITC–peptide (0–1000 μg). The amount of conjugated protein in the hydrogels was quantified by BCA assay kit (Thermo Fisher Scientific, Waltham, MA, USA). After protein–hydrogels were prepared, washed to remove unconjugated proteins for 3 hours. Washed buffer were collected and measure unconjugated proteins by BCA assay.

2.3.3 Preparation of 3D cell culture

In vitro 3D culture of hPDLSCs was carried out to examine cell proliferation in the peptide-hydrogel. For the 3D hPDLSC cultures, a total of 300 μ l of hydrogel was prepared in a 24-well plate as follows. (1) Cells were suspended in solution B at a density of 5×10^4 cells. (2) Solution B with suspended cells was mixed with solution A supplemented with CP, CBMP, or BMP-2. (3) α -MEM supplemented with 10 % FBS and 1 % antibiotic-antimycotic solution was added, and media was replaced every 1-2 days over a period of 14 days.

2.3.4 Cell proliferation in the peptide-hydrogel

To determine cell viability, hPDLSCs cultured in peptide or protein-hydrogel were maintained in α -MEM supplemented with 10 % FBS and 1 % antibiotic-antimycotic solution. The cell viability was determined using the DNA assay kit (Quant-iT™ PicoGreen dsDNA Assay Kit, Thermo Fisher Scientific, Waltham, MA, USA), Cell Counting Kit-8 (CCK-8, Dojindo Molecular Technologies, Tabaru, Japan), and LIVE/DEAD viability assay kit (Thermo Fisher Scientific, Waltham, MA, USA). Before the experiments, the hPDLSCs were encapsulated CP-, CBMP-, or BMP-2-hydrogel in 24-well plates and maintained for day 1, 3, 7, and 14.

For DNA quantification assay, The cultured cells were

recovered by selective degradation of hydrogels using 2.5–25 units per mL of collagenase treatment at 37 °C for 30 min. The solutions were centrifuged at 13000 rpm for 5 min to obtain cell pellets. The cells were lysed with 200 μ L of lysis buffer (M-PER™ Mammalian Protein Extraction Reagent, Thermo Fisher Scientific, Waltham, MA, USA), and the solutions were mixed with 200 μ L of PicoGreen working solution. Sample fluorescence was measured at an excitation wavelength of 480 nm and an emission wavelength of 520 nm.

For CCK–8 assay, the cells in the PBS, CP, CBMP, or BMP–2–hydrogel were incubated with 2–(2–methoxy–4–nitro–phenyl)–3–(4–nitrophenyl)–5–(2,4–disulfophenyl)–2H–tetrazolium, monosodium salt (WST–8) for 1 hour at 37°C. The intensity of the CCK product was measured at 450nm using microplate reader.

Also, cell death was examined by LIVE/DEAD viability assay kit (Thermo Fisher Scientific, Waltham, MA, USA). The cells were incubated with a mixture of 6 mM calcein AM and 4 mM ethidium homodimer–1 (EthD–1) at 37 °C for 30 min, and they were then imaged using a fluorescence microscope (FV300, Olympus, Tokyo, Japan).

2.3.5 Osteogenic potential of hPDLSCs cultured in peptide–hydrogel : Immunofluorescence assay

The hPDLSCs were cultured in hydrogels with CBMP, CP, or

BMP-2 in 4-well chambers and incubated at 37 °C, 5 % CO₂. On day 14, the cells were fixed with 10 % NBF for 10 min at room temperature. The cells were washed with DPBS and blocked with 3 % bovine serum albumin for 30 min at room temperature. The cells were incubated with primary antibodies (anti-Runx2 , anti-OCN (1:200)) in DPBS containing 3 % bovine serum albumin (BSA) for 16 hours at 4°C. After three washes, the cells were incubated with secondary antibodies (goat anti-mouse IgG-Rhodamine and goat anti-rabbit IgG-FITC 1:1000) in DPBS containing 3 % BSA for 1 hour, followed by another three washes and then for stain cell nuclei incubated with 4',6-diamidino-2-phenylindole (DAPI) (Thermo Fisher Scientific, Waltham, MA, USA) for 15min at room temperature. The cells were mounted with Faramount Aqueous Mounting Medium (DAKO, Glostrup, Denmark). The slides were observed using a confocal laser scanning microscope (FV300, Olympus, Tokyo, Japan). Total signal arising from cells were obtain average pixel intensity value using FV300.

2.3.6 Osteogenic differentiation of hPDLSCs in the peptide hydrogel : Quantitative real time polymerase chain reaction assay

The hPDLSCs were incubated in peptide or protein-hydrogel for 14 days in mineralization medium. At the end of the indicated time, the encapsulated cells were harvested using the collagenase treatment, as described for the DNA quantification

assay. Total RNA was isolated using TRIzol (Thermo Fisher Scientific, Waltham, MA, USA) and then quantified by ultraviolet (UV) spectroscopy. A cDNA library was synthesized using DNase I-treated total RNA (1 mg) by oligo dT priming using the Super Script II pre-amplification system (Thermo Fisher Scientific, Waltham, MA, USA). PCR (polymerase chain reaction) was performed using a GeneAmp PCR 9700 thermo cycler. Real-time quantitative PCR analysis was performed on an ABI PRISM 7500 (Applied Biosystems, CA, USA) by SYBR Green I dye detection. The reactions were performed according to the manufacturer's instructions. The PCR primer sequence were as shown in Table 1. and conditions were as follows: 10 s at 95 °C, followed by 30–35 cycles of 10 s at 95 °C, 10 s at the annealing temperature, and 10 s at 72 °C. The results were normalized to GAPDH (a housekeeping gene) as a reference gene, and relative gene expression levels were expressed as a fold change to the hPDLSCs cultured on the tissue culture plate (control). All reactions were performed in triplicate.

2.3.7 Osteogenic differentiation of hPDLSCs in the peptide-hydrogel : mineral detection by Energy dispersive spectrometer assay

At late-stage osteogenic differentiation, calcium deposition was also quantified using scanning electron microscope (SEM, S-4700, HITACHI, Tokyo, Japan)/Energy Dispersive Spectrometer (EDS, EMAX, HORIBA, Kyoto, Japan). For calcium

deposition quantification using EDS, the hydrogels were examined after the mineralization experiments. Cells were fixed in 4 % paraformaldehyde for 24 hours, followed by 1 % OsO₄ for 1 hour and 2 % tannic acid. Samples were then dehydrated in graded ethanol solutions followed by hydroxymethyl xylazine (HMSM), sputter-coated with gold palladium and examined in a SEM/EDS at an accelerating voltage of 15 kV and magnifications of 3,000x and 15,000x. SEM/EDS analysis was performed utilizing a SEM operating at 15 kV with attached Kevex EDS for demonstration of deposition of calcium and phosphate ions.

2.3.8 In vivo osteogenic activity of hPDLSCs in peptide-hydrogel

2.3.8.1 Surgical procedure of application of hPDLSCs peptide-hydrogel in the rat calvarial defect model

Sprague Dawley male rats weighing 250–300 g were used to assess the *in vivo* bone forming capacity of CBMP-hydrogel with hPDLSCs. The rats were anesthetized with Zoletil 50 (Virbac, Carros, France) and Rompun (Bayer AG, Leverkusen, German). A midline incision was made over the calvarium, and a full-thickness flap was elevated. A critically sized 8-mm calvarial defect was created using a trephine under sterile saline

irrigation. The animals were divided into five groups, as shown in Table 2, and treated with each method. The flaps were sutured by layer with 4-0 chromic gut and 4-0 silk. All the animals received a single intramuscular injection of cefazolin (Chong Kun Dang pharmaceutical corp., Seoul, Republic of Korea) (Fig. 1).

2.3.8.2 In vivo osteogenesis measured by micro-computed tomography analysis

Four weeks after implantation, the rats were sacrificed. Their skulls were harvested and fixed in 10 % NBF. The degree of bone formation at the critical-sized calvarial defects was estimated by micro-computed tomography (micro-CT, SkyScan 1172, Bruker, Billerica, MA, USA). The percent of bone volume and bone mineral density in each defect site was calculated using analysis software (CT analyzer, Bruker, Billerica, MA, USA).

2.3.8.3 Histological analysis of osteogenesis by hPDLSCs in the peptide-hydrogel applied in the calvarial defect

Following micro-CT scanning, each sample was decalcified in

Calci-Clear Rapid (National Diagnostics, Atlanta, GA, USA) for 2 weeks at room temperature on a rotating rocker. Following decalcification, samples were dehydrated overnight. Samples were then cut along the coronal plane at the midline of the defect and embedded in paraffin. Sections 5- μ m thick were mounted on individual slides and stained with hematoxylin and eosin stain and Masson's trichrome stain. Representative samples were evaluated for new bone formation.

2.4 Data analysis

All experiments were independently repeated at least three times. All values were expressed as the mean \pm S.D., and the means were compared using one-way ANOVA followed by Student's t-test. *P*-values of < 0.05 and < 0.001 were considered to be statistically significant.

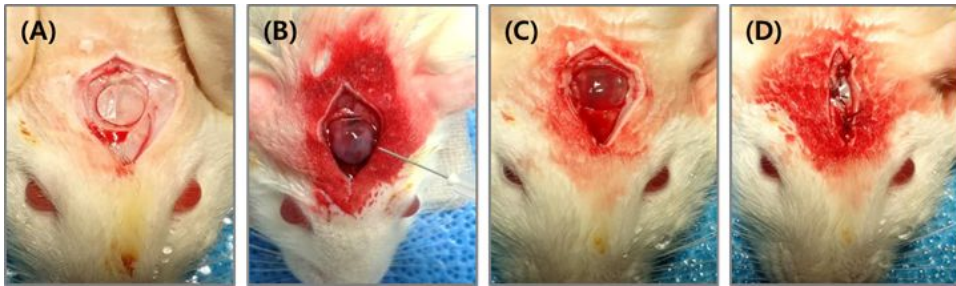


Figure 1. Surgical procedure of implanted hydrogel. (A) Creation of the critical size 8-mm defect in the rat calvarium. (B) Injection of biomolecule-conjugated hydrogels with hPDLSCs (C) Placement for the defected size. (D) Suturing the incised skin.

Table 1. The nucleotide sequences of the primers used for constructing osteogenic markers (alkaline phosphatase (ALP), runt-related transcription factor 2 (RUNX2), osteocalcin (OCN)) and housekeeping gene (glyceraldehyde 3-phosphate dehydrogenase (GAPDH))

Genes	GenBank No.	Primer sequence	Length (bp)
ALP	NM_000478.4	5'-cgggcacccatgaaggaaa-3'	184
		5'-ggccagaccaaaagatagagtt-3'	
RUNX2	NM_001024630.3	5'-ccgtccatccactctaccac-3'	139
		5'-atgaaatgcttggaactgc-3'	
OCN	NM_199173.5	5'-agctcaatccggactgt-3'	150
		5'-ggaagaggaaagaagggtgc-3'	
GAPDH	NM_001289746.1	5'-acatcatccctgcctctac-3'	171
		5'-ccaccttcttgatgtcatcatatttg-3'	

Table 2. Groups of the animal experiment of new bone formation. Used biomolecules were control peptide (CP), collagen binding motif peptide (CBMP), and bone morphogenetic protein(BMP)–2 for incorporation of hydrogel.

Name	PDLSCs/Gel	Bioactive molecule
No treatment	-	-
Empty gel	Gel only	-
CP	O	CP 5mM
CBMP	O	CBMP 5mM
BMP2	O	BMP2 100ng/ml

III. Results

3.1 CBMP synthesis and its osteogenic activity

The CBMP was synthesized using Fmoc chemistry and the synthesized CP, which had tyrosine in the original sequence changed to glutamine, served as a negative control. Peptide molecular weight and purity were assessed by LC/MS and HPLC, respectively. The CBMP and CP were obtained as the major synthesis products (purity \geq 98 %, Fig. 2). Using the LC / MS to confirm that the CBMP and CP were correctly synthesized measuring the molar weight. Mass spectra of CBMP was observed peak of $[\text{CBMP}+\text{H}]^{+2}$. To infer this peak, the synthesized CBMP molecular weight was 2262. Also, Mass spectra of CP was observed two peaks $[\text{CP}+2\text{H}]^{+2}$ and $[\text{CP}+3\text{H}]^{+3}$. To infer these peaks, the synthesized CP molecular weight was 2227.

To confirm osteogenic induced potential of synthesized CBMP, expression level of osteogenic markers was evaluated by western blot. Expression level of osteogenic proteins was examined at 14 days after peptide or protein transduction. Expression level of Runx2 and collagen type 1 was significantly higher under the CBMP treated condition than BMP-2, CP, or PBS treated cells. Expression level of OCN and pSmad1/5/8 increased under CP, CBMP, and BMP-2 treated condition compared with PBS treated condition. To compare CBMP and

BMP-2 treated condition, BMP-2 treated condition more increased pSmad1/5/8 expression. OPN was found to be equally expressed under CBMP and BMP-2 treated condition and expressed higher than CP and PBS treated condition (Fig. 3).

The ability of the synthesized CBMP on increased ALP activity and induced calcium deposits compared with the cells without treatment and cells treated with the CP, CBMP, and BMP-2 showed significantly increased formation of calcium phosphate crystals. The ALP activity assay showed that BMP-2 and CBMP increased ALP activity 2.4 and 2.0-fold compared with NT in OM condition (** $p < 0.05$, Fig. 4). Similarly, BMP-2 and CBMP induced expression 2.6 and 2.0-fold compared with NT in GM condition (* $p < 0.05$, Fig. 4).

Biominerals were quantified by alizarin red S stain. The alizarin red S stain assay showed that BMP-2 and CBMP were induced calcium deposition. Biominerals had increased 3.0-fold by BMP-2 and 2.7-fold by CBMP compared with NT cultured with OM (** $p < 0.05$, Fig. 5). In addition, BMP-2 and CBMP increased biominerals by 1.5 and 1.4-fold compared with NT cultured with GM (* $p < 0.05$, Fig. 5).

The calcified areas stain with ALP and alizarin red S was quantified (Fig. 4 and Fig. 5). The ability of the synthesized CBMP to induce osteogenic differentiation in hPDLSCs was determined to be similar to the osteogenic induction effect of BMP-2.

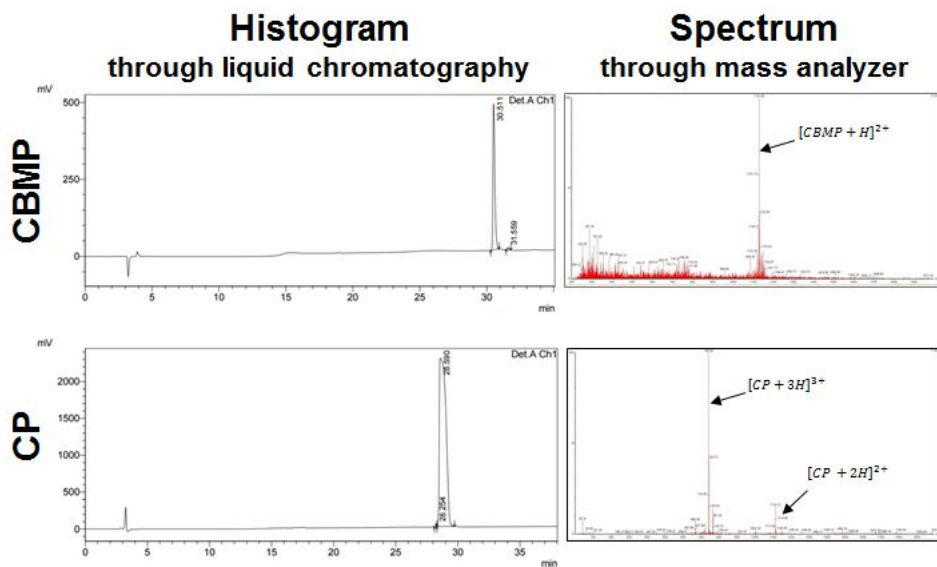


Figure 2. LC/MS results for collagen binding motif peptide (CBMP) and the control peptide (CP) after purification. The peak indicates the molecular weight of prepared peptide.

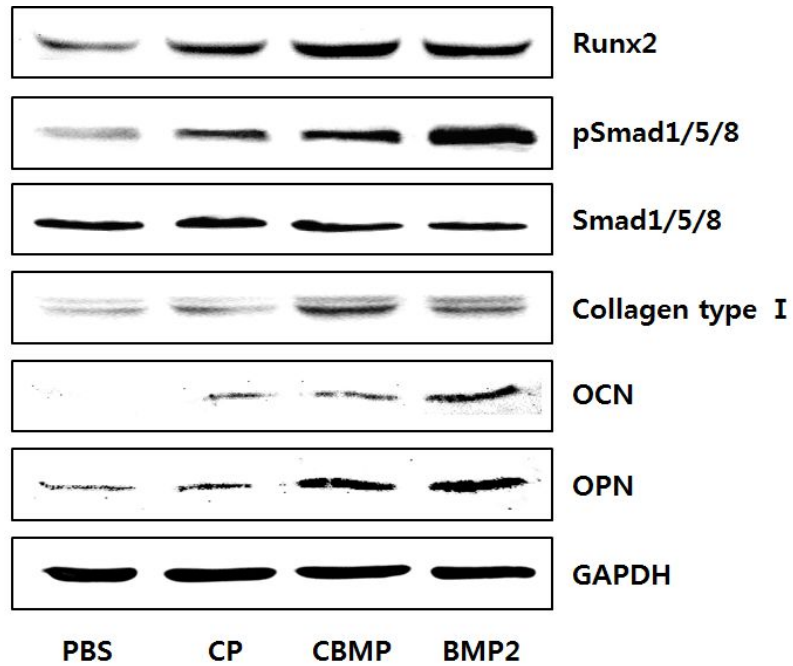


Figure 3. Osteogenic-specific protein expression induced by control peptide (CP), collagen binding motif peptide (CBMP), and bone morphogenetic protein (BMP)-2. The hPDLSCs were incubated with CBMP (100 μ M), CP (100 μ M), or BMP-2 (100 ng/ml), and the expression levels of osteogenic markers (Runt-related transcription factor 2 (RUNX2), pSmad1/5/8, Smad1/5/8, collagen type I, osteocalcin (OCN), osteopontin (OPN)) representing hPDLSC differentiation and mineralization, were detected by western blot.

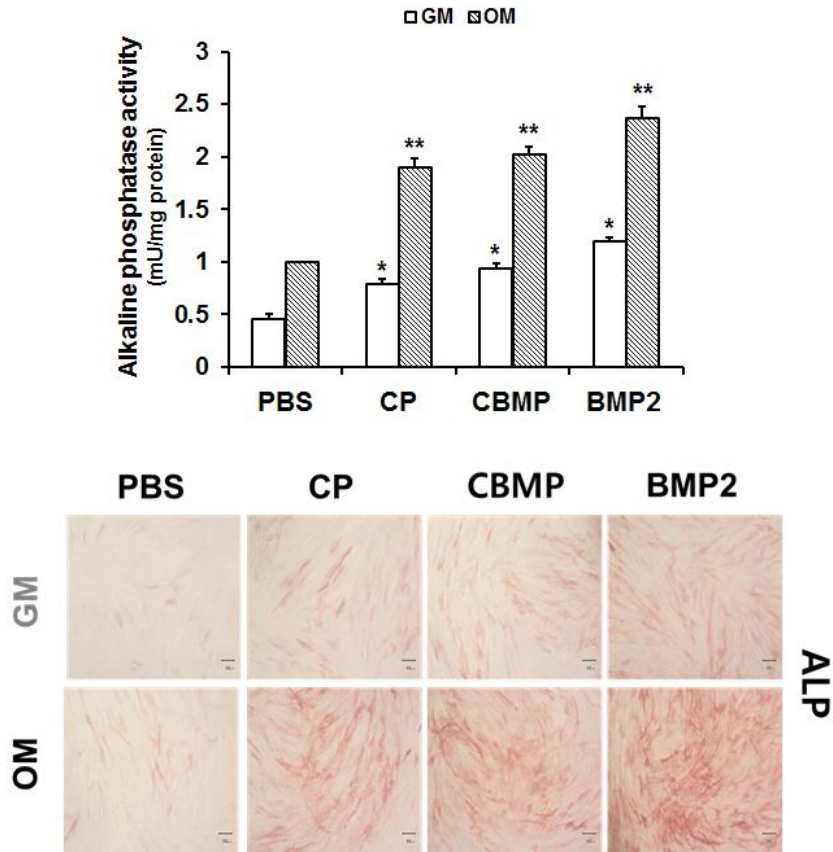


Figure 4. The alkaline phosphatase (ALP) activity assay. hPDLSCs were grown to confluence in 24-well culture plates and incubated with collagen binding motif peptide (CBMP) (100 μ M), control peptide (CP, 100 μ M), or bone morphogenetic protein (BMP)-2 (100 ng/ml) for 7 days in growth medium (GM) and osteogenic medium (OM). Osteogenic differentiation was induced by biomolecules. The hPDLSCs were treated with biomolecules for 14 days in growth or osteogenic media and then activity of the ALP enzyme in the media was detected. (* $p < 0.05$ as compared with PBS in GM. ** $p < 0.05$, as compared with PBS in OM.)

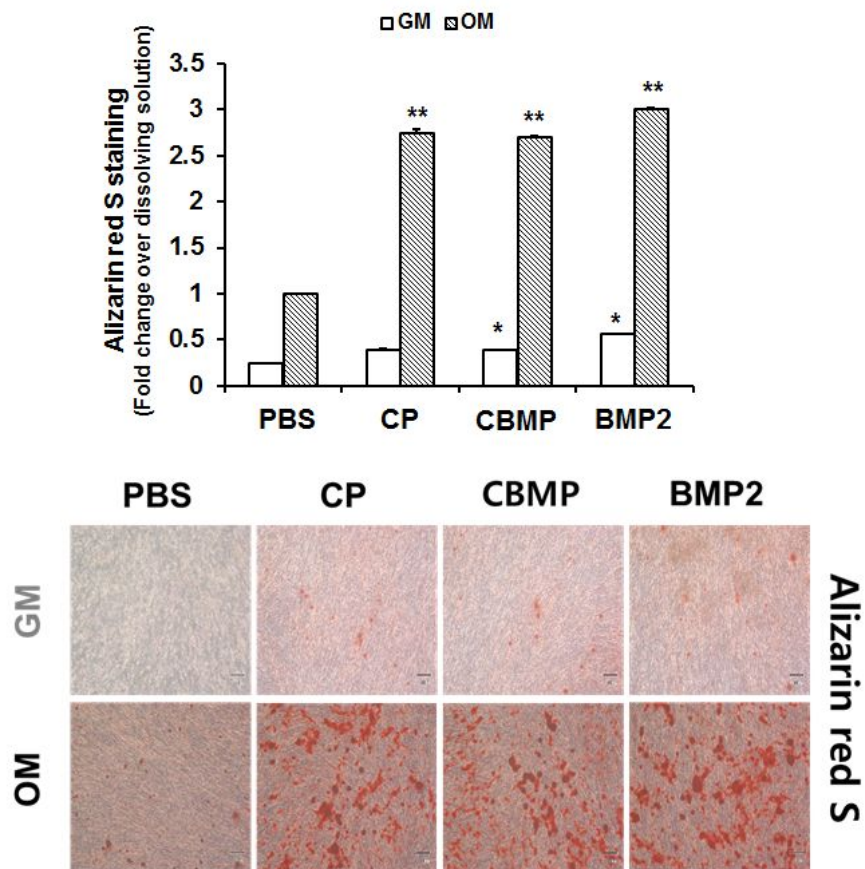


Figure 5. The alizarin red S assay. Osteogenic differentiation was induced by biomolecules. hPDLSCs were grown to confluence in 24-well culture plates and incubated with collagen binding motif peptide (CBMP) (100 μ M), control peptide (CP, 100 μ M), or bone morphogenetic protein (BMP)-2 (100 ng/ml) for 14 days in growth medium (GM) and osteogenic medium (OM). Osteogenic differentiation was induced by biomolecules. The hPDLSCs were treated with biomolecules for 14 days in GM or OM and then stained for alizarin red S. (* p < 0.05 as compared with PBS in GM. ** p < 0.05, as compared with PBS in OM.)

3.2 Peptide conjugated hydrogel

3.2.1 Incorporation efficiency of peptide in the hydrogel

Peptide-conjugated hydrogel was formed with 1 mg peptide or 100 ng protein per 1 mL hydrogel to evaluate the effect of the peptide on conjugation efficiency. The CBMP-hydrogel conjugation efficiency was 81 % (0.81 mg/gel). The BMP-2 and hydrogel conjugation efficiency was 29 % (29 ng/gel). The CP-hydrogel conjugation efficiency was 12 % (0.12 mg/gel) due to the lack of phenol molecules in peptide (Fig. 6, Table 3).

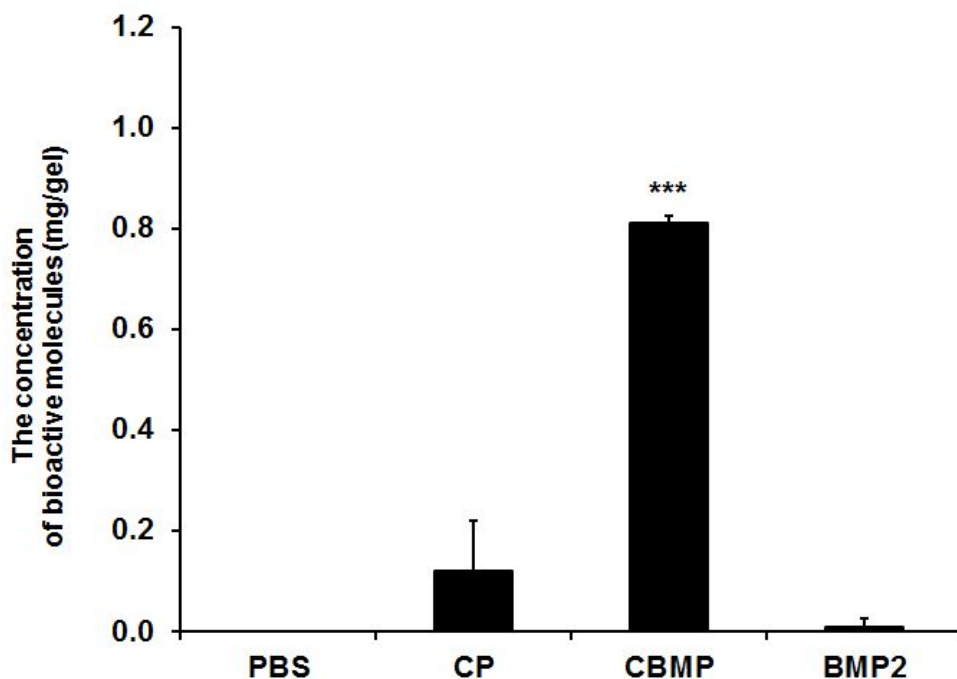


Figure 6. Biomolecule concentrations within the hydrogels as a function of the feed peptide concentration. Hydrogels conjugated peptide in the hydrogels was quantified by relative fluorescence unit (RFU) intensity using FITC-peptides. FITC-peptide-hydrogels were prepared as previously described of control peptide (CP) and collagen binding motif peptide (CBMP). They were then washed to remove unconjugated peptides for 3 hours. The hydrogel samples were imaged using an LAS-1000 CCD camera. In case of bone morphogenetic protein (BMP)-2-hydrogels, hydrogel were washed to remove unconjugated proteins for 3 hours. Washed buffer were collected and measure unconjugated proteins by BCA assay. (***) $p < 0.001$ as compared with PBS.)

Table 3. Groups of incorporation efficiency experiment of PBS-, control peptide (CP)-, collagen binding motif peptide (CBMP)-, and bone morphogenetic protein (BMP)-2-hydrogel.

Sample name	polymer conc. (wt%)	Bioactive molecule conc. (mg/mL)	Conjugation efficacy (%)
PBS	5	-	-
CP	5	5	11.9 ± 5.1
CBMP	5	5	81.2 ± 0.2
BMP2	5	0.0001	28.6 ± 1.4

3.2.2 Evaluation of cell proliferation in a 3D environment

The proliferation of hPDLSCs in the CBMP-, CP-, BMP-2-hydrogel was examined by dsDNA content assay and LIVE/DEAD viability assay measurements. The majority of the cells in all hydrogels were viable (stained green) after 1, 3, 7, and 14 days of culture, and dead cells were scarcely detected (stained red) (Fig. 7). The cells were no significant change in cell growth and death for cultured in CP-, CBMP-, and BMP-2-hydrogel compared with PBS-hydrogel.

The density of cells proliferating in the hydrogel was quantitatively measured using the CCK-8 assay. Cells were seeded on day 0 with PBS-, CP-, CBMP-, and BMP-2-hydrogel. The cell proliferation was analysis on days 1, 3, 7, and 14. The cells were found to be equally proliferative in the untreated, within peptide, or protein conjugated hydrogel environment (Fig. 8).

Also, cell proliferation was confirmed by DNA contents assay. Analysis of cell proliferation in hydrogel condition compared the initial DNA content of seeded cells on day 0 with that of cells on days 1, 3, 7, and 14. The DNA contents were found to be equally value in the untreated, within peptide, or protein conjugated hydrogel environment (Fig. 9). These results indicate that the hydrogels were compatible to hPDLSCs, and that CBMP administration could be a safe *in vitro* and *in vivo* osteogenic procedure.

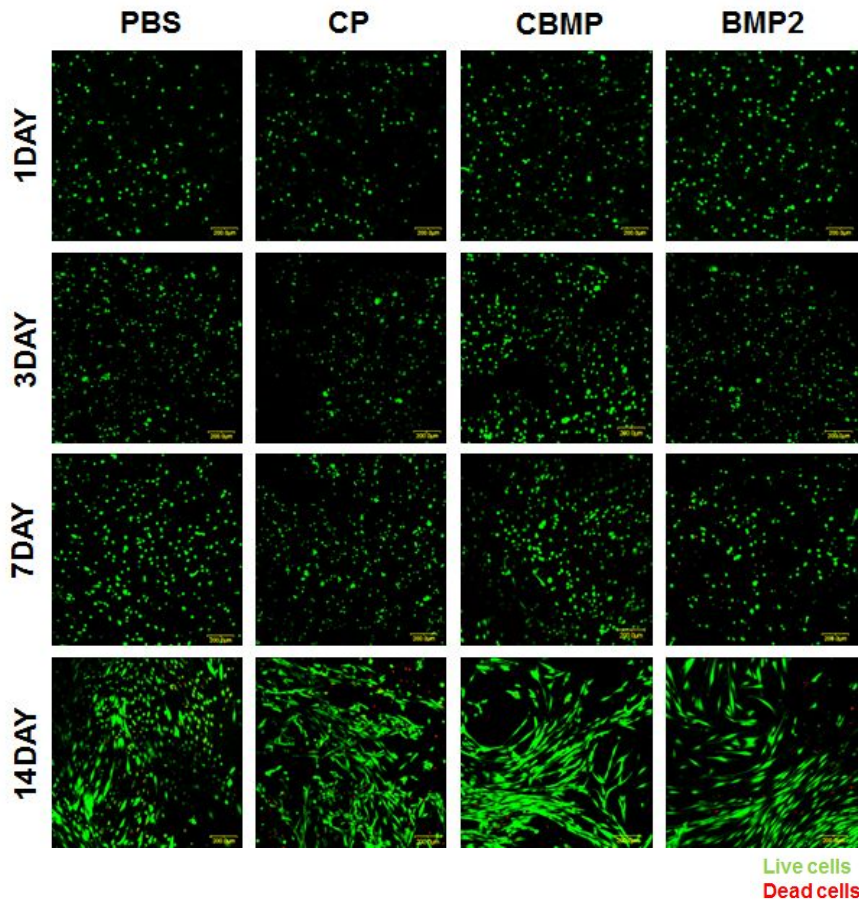


Figure 7. Effect of PBS, control peptide (CP), collagen binding motif peptide (CBMP), or bone morphogenetic protein (BMP)–2 incorporation on viability of the hPDLSCs cultured in hydrogels. The cells were cultured in the hydrogel 3D environment for 2 weeks, and viability was assessed at days 1, 3, 7, and 14 using the LIVE/DEAD assay (scale bar=200 μ m). The cells were incubated with a mixture of 6 mM calcein AM and 4 mM ethidium homodimer–1 at 37 °C for 30 min, and they were then imaged using a fluorescence microscope (FV300, Olympus, Tokyo, Japan). Representative LIVE/DEAD images are shown for each time point.

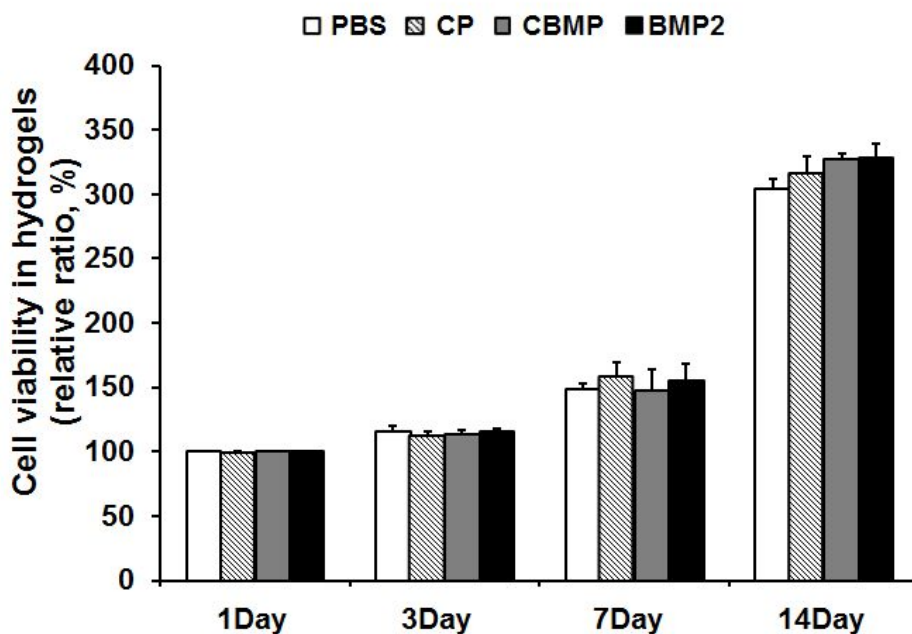


Figure 8. Proliferation of 3D cultured hPDLSCs. CCK-8 assays were performed to determine cell viability with PBS, control peptide (CP), collagen binding motif peptide (CBMP), and bone morphogenetic protein (BMP)-2. The cells in the peptide or protein-hydrogel were incubated with WST-8 for 1 hour at 37 °C. Cells cultured for 1, 3, 7 and 14 days was measured using the CCK-8 assay. The intensity of the CCK product was measured at 450nm using microplate reader.

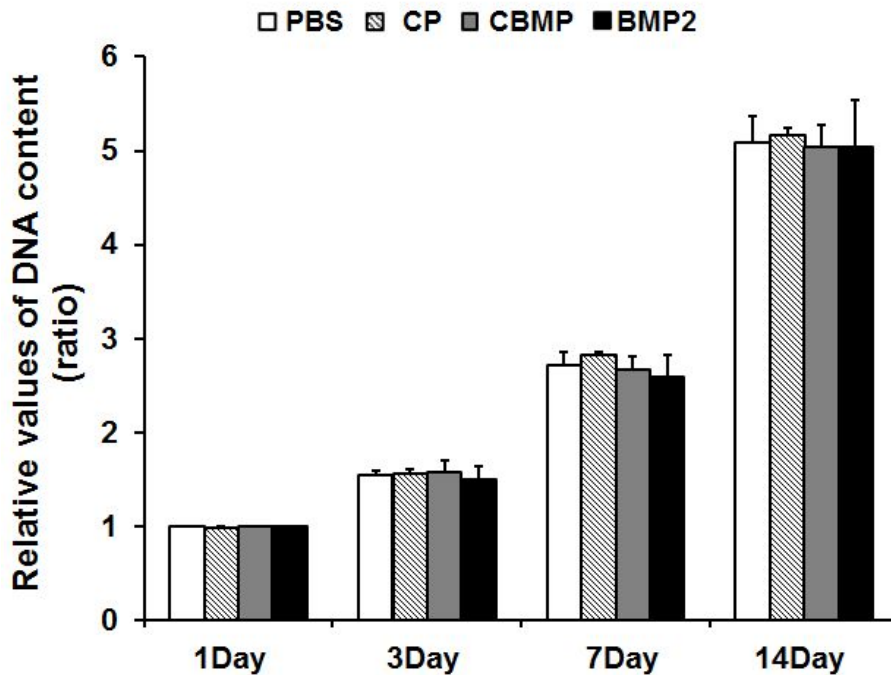


Figure 9. Proliferation of 3D-cultured hPDLSCs. Cells cultured in PBS-, control peptide (CP)-, collagen binding motif peptide (CBMP)-, or bone morphogenetic protein (BMP)-2-hydrogel were recovered by selective degradation of hydrogels using 2.5-25 units per mL of collagenase treatment. The cells were lysed with 200 μ L of lysis buffer, and the lysates were mixed with PicoGreen working solution. Sample fluorescence was measured. The total DNA isolated from 3D constructs cultured for 1, 3, 7 and 14 days was measured using the PicoGreen assay.

3.2.3 Peptide-conjugated hydrogel for osteogenic ability

The efficiency of CBMP-hydrogel in osteoinduction was monitored at the protein level using immunofluorescence assay. After 14 days, Runx2 and OCN protein levels were induced. Intensity of FITC (Runx2) and rhodamine (OCN) was significantly higher in the CBMP-hydrogel than PBS-, CP-, BMP-2-hydrogel (Fig. 10). In detail, expression level of Runx2 increased 2-fold by CP-hydrogel, 7.5-fold by CBMP-hydrogel, and 4-fold by BMP-2-hydrogel compared with PBS-hydrogel. Also, expression level of OCN increased 2.7-fold by CP-hydrogel, 6.1-fold by CBMP-hydrogel, and 3.2-fold by BMP-2-hydrogel compared with PBS-hydrogel (Fig. 11). This effect was accompanied by a significant increase of the expression of the master regulators of osteogenesis, Runx2 and OCN.

To understand the action of CBMP on the hPDLSCs at the molecular level, osteogenic gene expression marker including ALP, OCN, and Runx2 were measured. Quantitative real-time PCR analysis showed that both OCN and Runx2 expression increased during osteogenic differentiation in CBMP-hydrogels compared with those observed in CP-hydrogels and BMP-2-hydrogels (Fig. 12). In detail, expression level of Runx2 mRNA increased 1.4-fold by CP-hydrogel, 3.3-fold by CBMP-hydrogel, and 3.8-fold by BMP-2-hydrogel compared with PBS-hydrogel ($*p < 0.05$). Expression level of ALP mRNA increased 1400-fold by CP-hydrogel, 2800-fold by

CBMP-hydrogel, and 1300-fold by BMP-2-hydrogel compared with PBS-hydrogel ($*p < 0.05$). Also, expression level of OCN mRNA increased 2-fold by CBMP-hydrogel and 1.5-fold by BMP-2-hydrogel compared with PBS-hydrogel ($*p < 0.05$, Fig. 12). This evidence suggests that the CBMP-hydrogel has osteogenic potential.

Matrix mineralization was assessed using SEM/EDS. Calcium deposit formation was examined. After day 14 in culture, the formation of mineralized nodules was observed. The SEM images of calcium deposits at 14 days indicate that CBMP-hydrogels enhanced matrix deposition and mineralization compared with PBS-, CP-, and BMP-2-hydrogels (Fig. 13). EDS spectra of mineralization showed that peaks of calcium and phosphate ions indicative of deposition in CP-, CBMP-, and BMP-2-hydrogel and each Ca/P ratio was 0.75, 1.47, 1.52, and 1.32 (Table 4). This result demonstrates the bioactive nature of the composite scaffolds.

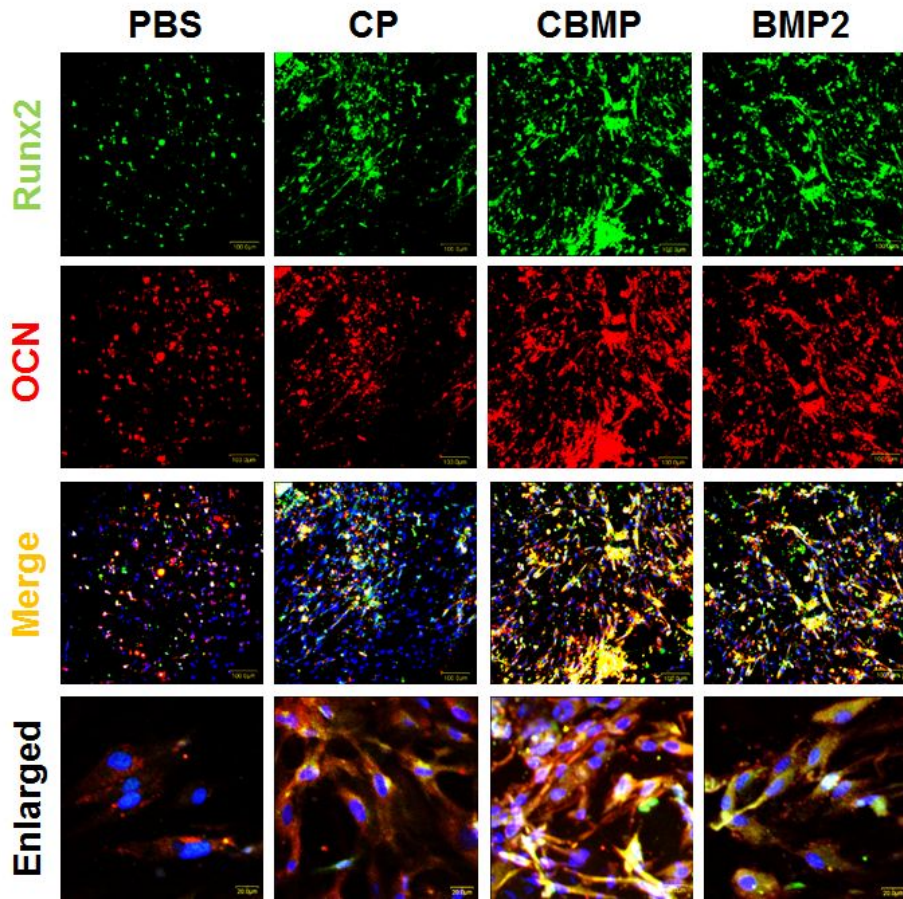


Figure 10. The hPDLSCs cultured in osteogenic medium (OM) for 14 days expressed runt-related transcription factor 2 (Runx2, green) and osteocalcin (OCN, red). The hPDLSCs were cultured in hydrogels with PBS, collagen binding motif peptide (CBMP), control peptide (CP), or BMP-2 in 4-well chambers and incubated. When cultured in OM for 14 days, hPDLSCs strongly expressed Runx2 and OCN as shown by immunofluorescent staining. Cell nuclei were stained with DAPI. The magnifications shown are 200x and 800x.

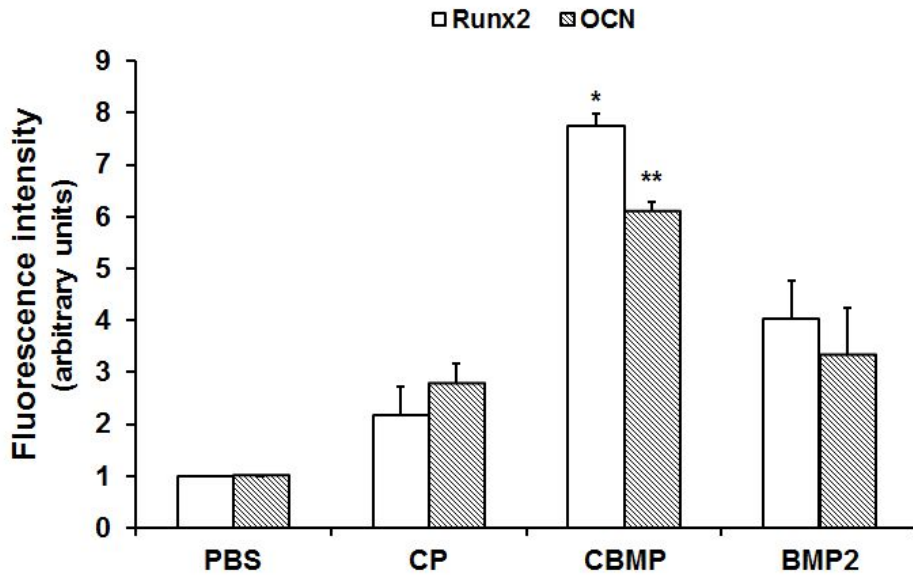


Figure 11. Fluorescence intensities of runt-related transcription factor 2 (Runx2) and osteocalcin (OCN) in PBS, control peptide (CP), collagen binding motif peptide (CBMP), and bone morphogenetic protein (BMP)-2 treated groups. After taking images, total signal arising from cells were obtain average pixel intensity value using FV300. Quantified fluorescence microscopy results are shown. (* $p < 0.05$ as compared with PBS in Runx2. ** $p < 0.05$, as compared with PBS in OCN.)

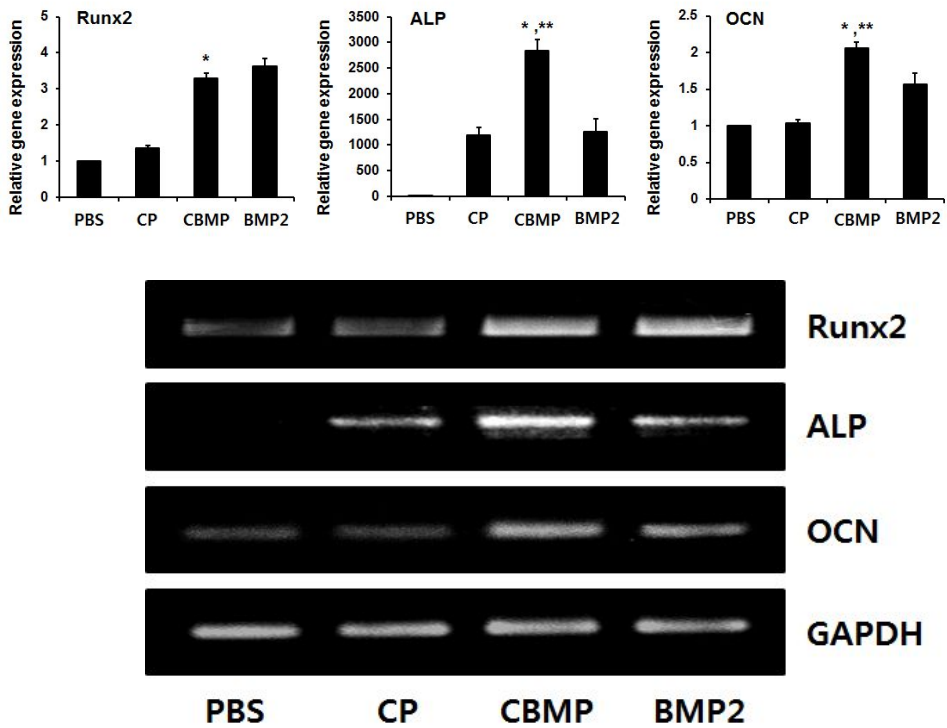


Figure 12. Analysis of peptide-hydrogel osteoinductivity with hPDLSCs. The hPDLSCs were incubated in PBS-, control peptide (CP)-, collagen binding motif peptide (CBMP)-, and bone morphogenetic protein (BMP)-2-hydrogel for 14 days in mineralization medium. the encapsulated cells were harvested using the collagenase treatment, total RNA was isolated and then a cDNA library was synthesized. Real-time quantitative PCR analysis was performed by SYBR Green I dye detection. The mRNA levels of alkaline phosphatase (ALP), osteocalcin (OCN), and runt-related transcription factor 2 (RUNX2) at day 14 of hPDLSC osteogenic differentiation are shown, as determined by real-time PCR. (* $p < 0.05$ as compared with PBS. ** $p < 0.05$, as compared with BMP-2)

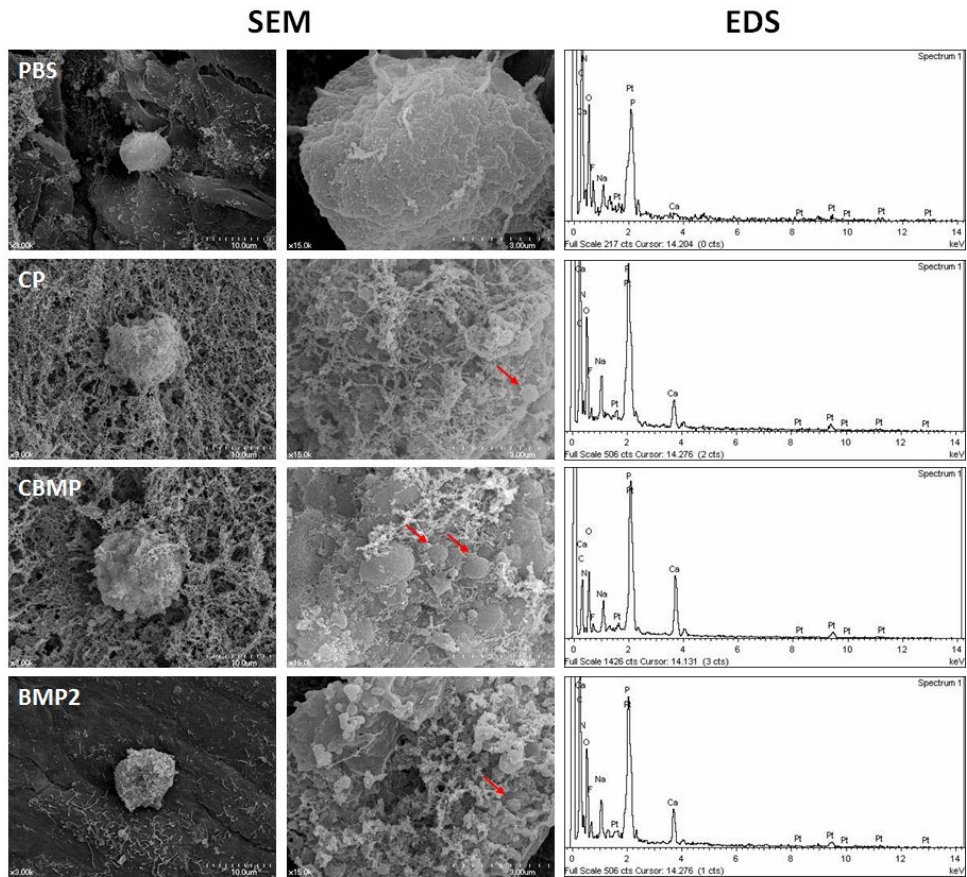


Figure 13. Mineralization of hPDLSCs in a PBS–, control peptide (CP)–, collagen binding motif peptide (CBMP)–, and bone morphogenetic protein (BMP)–2–hydrogel, as shown by SEM and EDS element analysis (arrow indicates the biominerals). Note clear peaks of calcium (Ca) in CBMP–hydrogel compared with PBS–, CP–, and BMP–2–hydrogel

Table 4. Surface elemental analysis of hydrogels by EDS with platinum, osmium, fluorine, and sulphur. Calcium (Ca) and phosphorus (P) were detected on surfaces of PBS-, control peptide (CP)-, collagen binding motif peptide (CBMP)-, and bone morphogenetic protein (BMP)-2-hydrogel

%	C	Na	P	Ca	etc.	total	Ca/P
PBS	30.77	1.28	0.68	0.51	33.01	100	0.75
CP	27.25	2.31	2.90	4.26	21.77	100	1.47
CBMP	17.45	2.97	7.36	11.21	30.61	100	1.52
BMP2	26.38	2.77	4.92	6.49	21.85	100	1.32

3.2.4 New bone formation by the hPDLSCs in the peptide-hydrogel

Typical 3D images are shown in Fig. 14. New bone formation was clearly advanced in defects treated with hPDLSCs in CBMP-hydrogel. In the group without treatment, dense and fibrous connective tissue at the defect site was observed. No severe inflammatory reaction was observed in untreated groups. The group treated with hydrogel showed little bone formation from the defect, similar to the group without treatment. Connective tissue rather than new osteoid was evident in the specimens treated with CP-hydrogel. However, in the group treated with CBMP-hydrogel, the new bone formation was marked, bone growth starting from the bony borders toward the center of the defect. In addition, in the group treated with BMP-2-hydrogel, the new bone formation was marked but less than CBMP-hydrogel.

Histological specimens were taken to examine no treatment, PBS-, CP-, CBMP-, and BMP-2-hydrogel. The no treatment and PBS-hydrogel groups exhibited minimal mineralized regions, and the mineralized regions were confined mostly to the defect edge. CP-hydrogel displayed small patches of mineralization. In contrast, CBMP- and BMP-2-hydrogel demonstrated multiple layers and islets of dispersed irregularly shaped mineralized regions within the treated region. In addition, the CBMP-hydrogel appeared to have had more ingrowth of mineralized areas from the defect edge, relative to the PBS group, hydrogel, CP-, and BMP-2-hydrogel (Fig. 14, Fig. 16,

and Fig. 17). Both micro-CT and histology results showed that bone formation area and bone mineral density (BMD) of CBMP-hydrogel ($12.3 \pm 1.4 \text{ mm}^3$, $0.1 \pm 0.01 \text{ g/cm}^2$) were higher than that of BMP-2-hydrogel ($8.5 \pm 1.6 \text{ mm}^3$, $0.077 \pm 0.002 \text{ g/cm}^2$) (Fig. 15). Bone formation within CBMP-hydrogel was qualitatively and quantitatively superior to that obtained with scaffolds containing CP- or BMP-2-hydrogel defects.

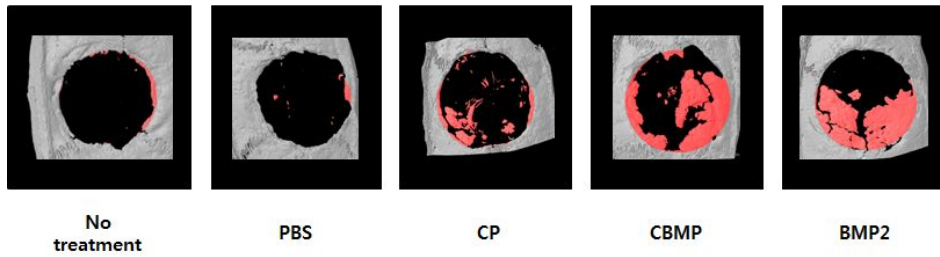


Figure 14. 3D micro-CT images were reconstructed using analysis software. Calvarial defect models were implantation of no treatment, PBS-, control peptide (CP)-, collagen binding motif peptide (CBMP)-, and bone morphogenetic protein (BMP)-2-hydrogel. After 4 weeks from implanted, rats were sacrificed and estimated by micro-CT. The red area indicates the regeneration bone area

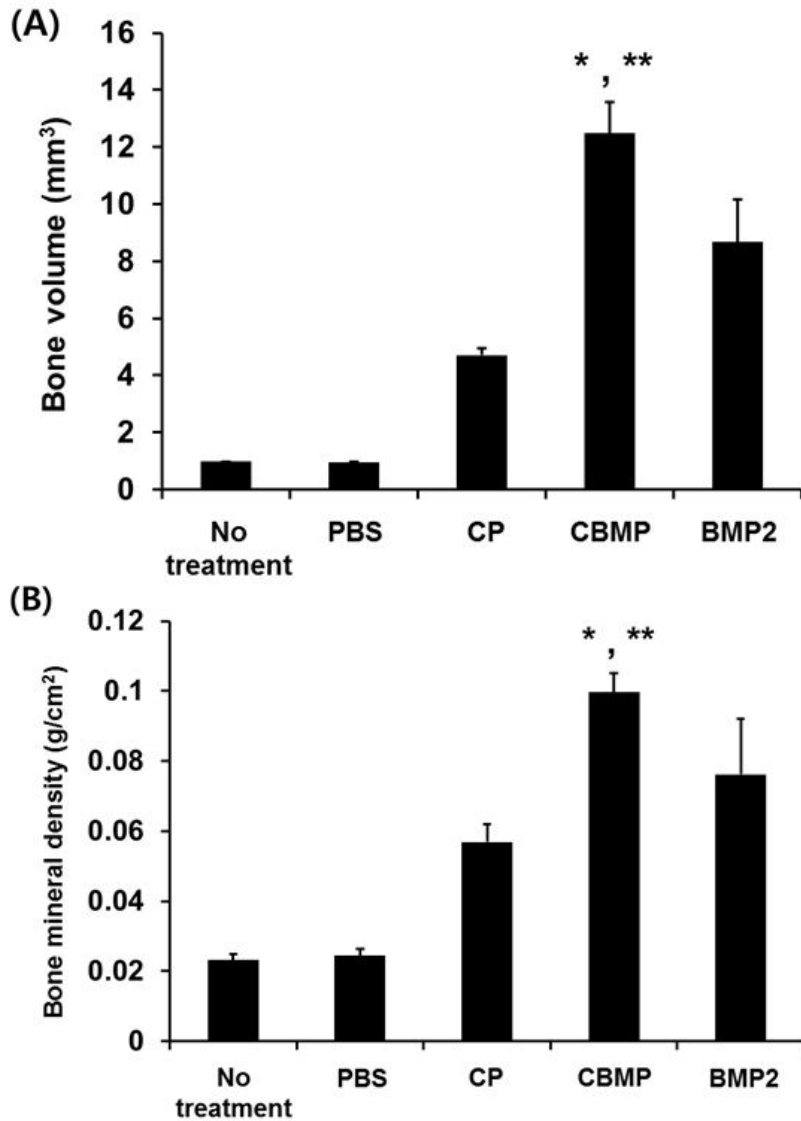


Figure 15. The no treatment, PBS, control peptide (CP), collagen binding motif peptide (CBMP), and bone morphogenetic protein (BMP)-2 groups were measured for bone volume (A) and bone mineral density (B). BMD were prepared as different density of phantom. (* $p < 0.01$ as compared with PBS, ** $p < 0.01$ as compared with BMP-2.)

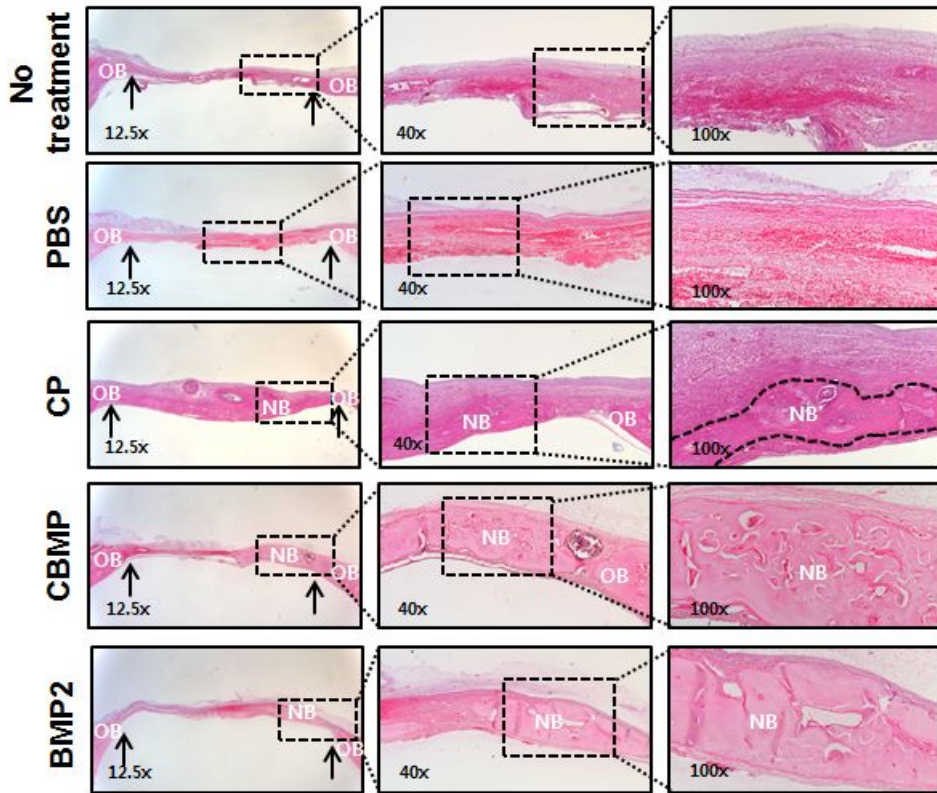


Figure 16. Representative H&E stained histological sample obtained 4 weeks post-surgery from rats that received hydrogel implants. Untreatment group (original magnification 12.5x, 40x, 100x), PBS-hydrogel group (original magnification 12.5x, 40x, 100x), control peptide (CP)-hydrogel (original magnification 12.5x, 40x, 100x), collagen binding motif peptide (CBMP)-hydrogel group (original magnification 12.5x, 40x, 100x), bone morphogenetic protein (BMP)-2-hydrogel group (original magnification 12.5x, 40x, 100x). (OB = old bone, NB = new bone, arrow indicates the boundary between old and new bone)

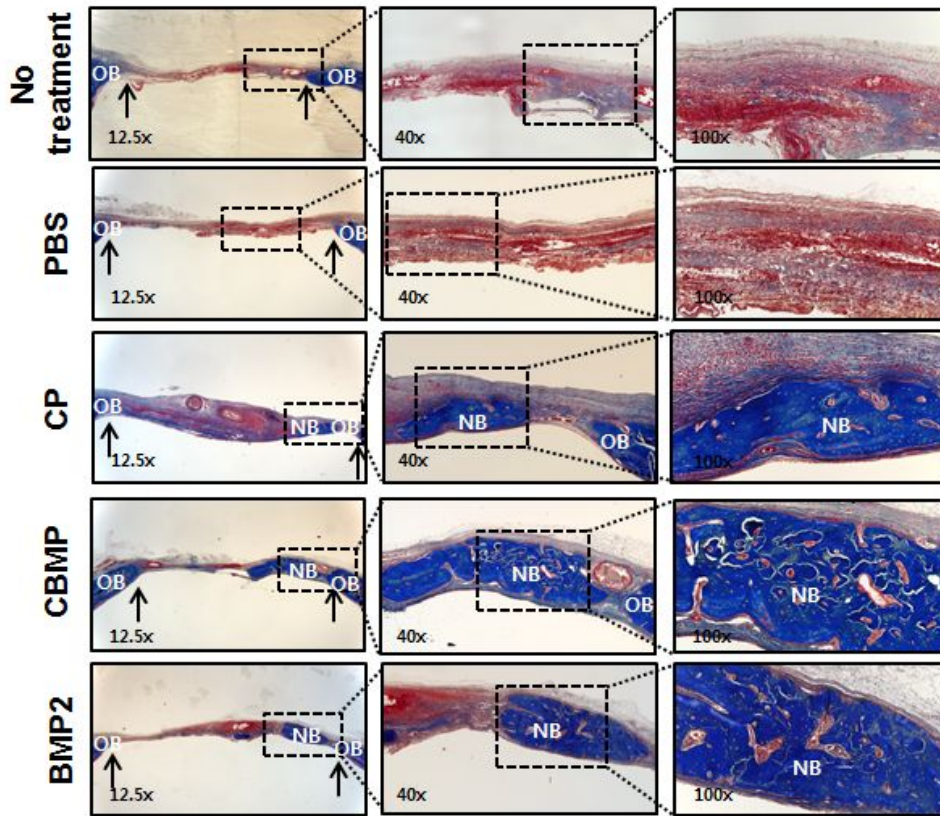


Figure 17. Representative Masson's trichrome stained histological sample obtained 4 weeks post-surgery from rats that received hydrogel implants. Untreatment group (original magnification 12.5x, 40x, 100x), PBS-hydrogel group (original magnification 12.5x, 40x, 100x), control peptide (CP)-hydrogel (original magnification 12.5x, 40x, 100x), collagen binding motif peptide (CBMP)-hydrogel group (original magnification 12.5x, 40x, 100x), bone morphogenetic protein (BMP)-2-hydrogel group (original magnification 12.5x, 40x, 100x). (OB = old bone, NB = new bone, arrow indicates the boundary between old and new bone.)

IV. Discussion & Conclusion

Biomaterials play a critical role in the success of tissue engineering, since they provide mechanical stability to the self-healing tissues and drive their shape and structure [1, 18]. Moreover, they can control and stimulate the regeneration of the living tissue itself by activating specific genes through their dissolution or, if required, releasing growth factors and drugs.

The injectable hydrogel is one of particular interest in various biomaterials because the hydrogels can be implanted through a facile process with minimal use of invasive surgical procedures. Thus, no surgical procedures are required for the implantation of hydrogels, or their removal in the case of the biodegradable ones. Hydrogels can be formed in situ either via chemical or physical cross-linking reaction mechanisms [19–21]. In this word, hydrogel easily modified with chemicals or drugs such as protein, peptide.

MSC-like cells can be isolated from periodontal ligament tissue and expanded in culture to generate populations with the properties expected of MSCs. Human PDLSC expanded ex vivo and seeded in three dimensional scaffolds were shown to generate bone [22–24]. These cells have also been shown to retain stem cell properties and tissue regeneration capacity.

Growth factors such as BMP are proven [25] and licensed therapies. However, lack of an efficient delivery vehicle requires application at supraphysiological doses to reach clinical efficacy. As well as stability, the application at supraphysiological doses

significantly increases the risk of side-effects, such as osteolysis, heterotopic ossification and swelling [26–27]. Peptides are small compared to large molecules such as proteins. Due to this smaller size, peptides can be easily synthesized, optimized and do not cause serious immune responses [28–30]. Peptides could be metabolically cleaved and rapidly cleared from body. Peptides do not accumulate in specific organs and this can minimize their toxic side effects. The region of the OPN was the only way to enhance osteogenesis.

In this study, CBMP from the collagen binding motif of OPN was synthesized, and its biological role in hPDLSCs was examined. This initial experiment attempted to determine whether this synthesized CBMP had osteogenic potential. The CBMP had potential of increase of osteogenic protein such as ALP, OPN, OCN, and Runx2 (Fig. 3). In addition, the CBMP increased ALP activity (Fig. 4) and induced calcium deposition (Fig. 5) similarly to BMP-2. The osteogenic potential of CBMP was almost similar to BMP-2. The CP which changed tyrosine to glutamine from CBMP also had osteogenic potential. The CP increased expression level of osteogenic proteins compared with PBS treated group (Fig. 3). The CP increased ALP activity and induced calcium deposition similarly to CBMP in GM and OM condition (Fig. 4 and Fig. 5). Therefore, CP could work control group in experiment of CBMP.

Incorporation efficiency of biomolecule-hydrogel was influenced by biomolecule. The mechanism of gelation was phenol-phenol crosslinking with H₂O₂ and HRP [22]. One of amino acids had phenol residue such as tyrosine. On the gelation, biomolecule which had tyrosine naturally crosslinked to hydrogel. The

hydrogel monomer and CBMP which had tyrosine were naturally crosslinked with H_2O_2 and HRP. However, incorporation efficiency of CP and hydrogel decreased due to absence of tyrosine. Though BMP-2 had eight tyrosines, incorporation efficiency was low (Fig. 6 and Table 3). According to previous studies, Almost tyrosines in BMP-2 were located in β -sheet [31] and in β -sheet, residues of amino acids were arranged inside or outside [32]. Also, chance of exposure of residue arranged in upper tertiary structure was declined [33]. For this reason, Probability of exposure of tyrosines in BMP-2 may low compared with CBMP which was secondary structure.

Proliferation of hPDLSCs as 3D culture was not any influenced by circumstance such as PBS-, CP-, CBMP-, and BMP-2-hydrogel. The cells in hydrogel were observed using calcein AM. The cells in CP-, CBMP-, and BMP-2-hydrogel were observed similarly to PBS-hydrogel control group (Fig. 7). In addition, the density of cells proliferating in the hydrogel was quantitatively measured using the CCK-8 assay and dsDNA content assay. Compared with PBS-hydrogel group, CP-, CBMP-, BMP-2-hydrogel groups were found to be equally proliferative (Fig. 8 and Fig. 9). In this reason hPDLSCs as 3D culture were not influenced by biomolecule-hydrogel.

The hPDLSC osteogenesis was enhanced by CBMP-conjugated hydrogels. These results suggest that CBMP-induced osteogenesis may result from controlling the lineage-specific transcriptional program based on inducing Runx2 gene expression (Fig. 10 and Fig. 12). Runx2 is the early and master transcription factor of the osteogenic transcriptional program, the initiation of which leads to up-regulation of various bone-related

genes and markers such as ALP, OCN. OCN is a late bone formation marker involved in constructing the bone matrix [34–37]. As shown in Fig. 10, Fig. 12, and Fig. 13, the CBMP–hydrogels induced OCN expression and calcium deposition more than the PBS–, CP–, and BMP–2–hydrogels. Table 4 shows that hPDLSCs in the CBMP–hydrogels deposited biominerals that exhibited a Ca/P ratio of 1.52, according to EDS measurements. The observed bone mineral Ca/P ratios ranged from 1.37–1.87 [38]. The Ca/P biominerals ratios induced by the CBMP–hydrogels are very similar to those of bone minerals. For this reason, the CBMP–hydrogel with hPDLSCs was induced osteogenesis and biominerals deposition like ossification.

Moreover, in the animal study, the CBMP–hydrogels showed better bone regeneration than the BMP–2–hydrogels. In the case of the BMP–2–hydrogels, BMP–2 is definitely a powerful biomolecule that can aid bone regeneration, but it has disadvantages. It strongly induced bone regeneration in the early phase, but it failed to induce a sustained, expanded bone regeneration due to protein stability *in vivo* [39]. The results showed minimal accumulation of calcium (Fig. 14). However, the CBMP–hydrogels aided bone regeneration much more than the BMP–2–hydrogels, and the resulting bone was much denser (Fig. 15B). The peptide–conjugated hydrogel, which constantly affected the defect areas, also induced dense new bone formation (Fig. 15A). Because peptide was more stable than protein, peptide worked sustainably [40]. Moreover, stained CBMP–hydrogel specimens show that new bone was formed more denser and more larger than CP–hydrogel and BMP–2–hydrogel specimen (Fig. 16 and Fig. 17). For this

reason, the CBMP–hydrogel with hPDLSC had potential of bone regeneration *in vivo*.

These study shows that the *in vivo* and *in vitro* bone–generating efficacy of CBMP, which is the region of the OPN–derived peptide, can greatly enhance the osteogenic differentiation of hPDLSCs and up–regulate osteogenic biomarkers. These results could have a great impact on osteogenesis and bone generation in dentistry and orthopedics. Further studies are necessary to assess the therapeutic potential of CBMP. These results provide new insight into using CBMP instead of BMP–2 as an osteogenic stimulator in further bone generation engineering clinical trials.

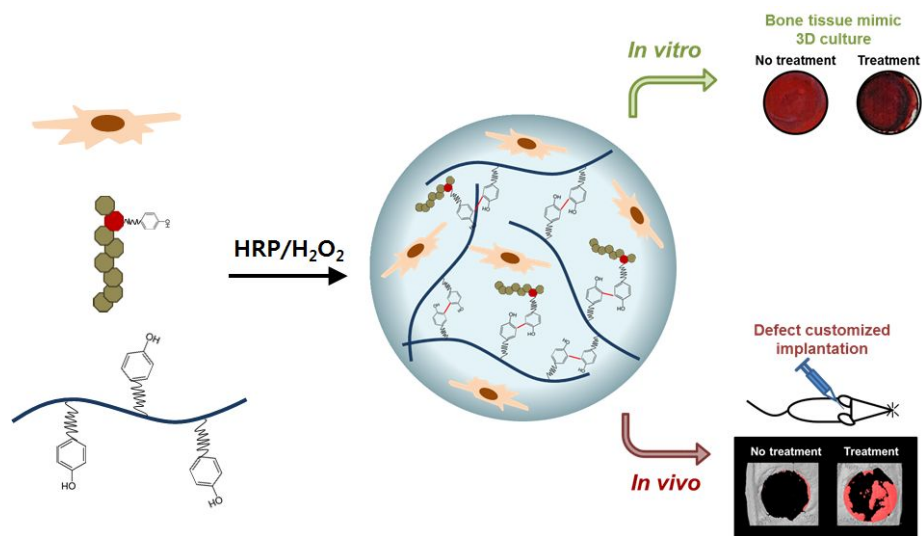


Figure 18. Schematic depicting the overall experimental model using the synthetic osteo-inductive peptide-conjugated hydrogel.

V. Reference

- [1] Park, K. M., Ko, K. S., Joung, Y. K., Shin, H., & Park, K. D. (2011). In situ cross-linkable gelatin-poly (ethylene glycol)-tyramine hydrogel via enzyme-mediated reaction for tissue regenerative medicine. *Journal of Materials Chemistry*, 21(35), 13180–13187.
- [2] Park, K. M., Lee, Y., Son, J. Y., Bae, J. W., & Park, K. D. (2012). In situ SVVYGLR peptide conjugation into injectable gelatin-poly (ethylene glycol)-tyramine hydrogel via enzyme-mediated reaction for enhancement of endothelial cell activity and neo-vascularization. *Bioconjugate chemistry*, 23(10), 2042–2050.
- [3] Han, F., Zhou, F., Yang, X., Zhao, J., Zhao, Y., & Yuan, X. (2014). A pilot study of conically graded chitosan-gelatin hydrogel/PLGA scaffold with dual-delivery of TGF- β 1 and BMP-2 for regeneration of cartilage-bone interface. *Journal of Biomedical Materials Research Part B: Applied Biomaterials*.
- [4] Karamzadeh, R., & Eslaminejad, M. B. (2013). *Dental-Related Stem Cells and Their Potential in Regenerative Medicine*.
- [5] Futaki, S., Suzuki, T., Ohashi, W., Yagami, T., Tanaka, S., Ueda, K., & Sugiura, Y. (2001). Arginine-rich peptides An abundant source of membrane-permeable peptides having potential as carriers for intracellular protein

delivery. *Journal of Biological Chemistry*, 276(8), 5836–5840.

- [6] Vila, A., Sanchez, A., Tob ı o, M., Calvo, P., & Alonso, M. J. (2002). Design of biodegradable particles for protein delivery. *Journal of Controlled Release*, 78(1), 15–24.
- [7] Batalia, M. A., & Collins, E. J. (1997). Peptide binding by class I and class II MHC molecules. *Peptide Science*, 43(4), 281–302.
- [8] Jha, A. K., Jackson, W. M., & Healy, K. E. (2014). Controlling osteogenic stem cell differentiation via soft bioinspired hydrogels.
- [9] Davis, M. E., Motion, J. M., Narmoneva, D. A., Takahashi, T., Hakuno, D., Kamm, R. D. & Lee, R. T. (2005). Injectable self-assembling peptide nanofibers create intramyocardial microenvironments for endothelial cells. *Circulation*, 111(4), 442–450.
- [10] Lee, J. Y., Choo, J. E., Choi, Y. S., Park, J. B., Min, D. S., Lee, S. J., ... & Park, Y. J. (2007). Assembly of collagen-binding peptide with collagen as a bioactive scaffold for osteogenesis in vitro and in vivo. *Biomaterials*, 28(29), 4257–4267.
- [11] Lee, J. Y., Choo, J. E., Park, H. J., Park, J. B., Lee, S. C., Jo, I., ... & Park, Y. J. (2007). Injectable gel with synthetic collagen-binding peptide for enhanced osteogenesis in vitro and in vivo. *Biochemical and biophysical research communications*, 357(1), 68–74.

- [12] Park, Y. S., Lee, J. Y., Suh, J. S., Jin, Y. M., Yu, Y., Kim, H. Y., ... & Jo, I. (2014). Selective osteogenesis by a synthetic mineral inducing peptide for the treatment of osteoporosis. *Biomaterials*, 35(37), 9747–9754.
- [13] Censi, R., Dubbini, A., & Matricardi, P. (2015). Bioactive hydrogel scaffolds—advances in cartilage regeneration through controlled drug delivery. *Current pharmaceutical design*, 21(12), 1545–1555.
- [14] Jin, G., Prabhakaran, M. P., & Ramakrishna, S. (2014). Photosensitive and Biomimetic Core-Shell Nanofibrous Scaffolds as Wound Dressing. *Photochemistry and photobiology*, 90(3), 673–681.
- [15] Diwan, M., & Park, T. G. (2001). Pegylation enhances protein stability during encapsulation in PLGA microspheres. *Journal of Controlled Release*, 73(2), 233–244.
- [16] Seo, B. M., Miura, M., Gronthos, S., Bartold, P. M., Batouli, S., Brahim, J., ... & Shi, S. (2004). Investigation of multipotent postnatal stem cells from human periodontal ligament. *The Lancet*, 364(9429), 149–155.
- [17] Fields, G. B., & Noble, R. L. (1990). Solid phase peptide synthesis utilizing 9-fluorenylmethoxycarbonyl amino acids. *International journal of peptide and protein research*, 35(3), 161–214.
- [18] Haid, R. W., Branch, C. L., Alexander, J. T., & Burkus, J. K. (2004). Posterior lumbar interbody fusion using recombinant human bone morphogenetic protein type 2

with cylindrical interbody cages. *The Spine Journal*, 4(5), 527–538.

- [19] Alonso, N., Risso, G. H., Denadai, R., & Raposo–Amaral, C. E. (2014). Effect of maxillary alveolar reconstruction on nasal symmetry of cleft lip and palate patients: A study comparing iliac crest bone graft and recombinant human bone morphogenetic protein–2. *Journal of Plastic, Reconstructive & Aesthetic Surgery*, 67(9), 1201–1208.
- [20] Gu, Y., Huang, W., Rahaman, M. N., & Day, D. E. (2013). Bone regeneration in rat calvarial defects implanted with fibrous scaffolds composed of a mixture of silicate and borate bioactive glasses. *Acta biomaterialia*, 9(11), 9126–9136.
- [21] Lieberman, J. R., Daluiski, A., Stevenson, S., JOLLA, L., WU, L., McALLISTER, P. A. U. L. A., ... & WITTE, O. N. (1999). The Effect of Regional Gene Therapy with Bone Morphogenetic Protein–2–Producing Bone–Marrow Cells on the Repair of Segmental Femoral Defects in Rats*. *The Journal of Bone & Joint Surgery*, 81(7), 905–17.
- [22] Oudgenoeg, G., Hilhorst, R., Piersma, S. R., Boeriu, C. G., Gruppen, H., Hessing, M., ... & Laane, C. (2001). Peroxidase–mediated cross–linking of a tyrosine–containing peptide with ferulic acid. *Journal of Agricultural and Food Chemistry*, 49(5), 2503–2510.
- [23] Boeriu, C. G., Oudgenoeg, G., Spekking, W. T. J., Berendsen, L. B., Vancon, L., Boumans, H., ... & Voragen, A. G. (2004). Horseradish peroxidase–catalyzed

- cross-linking of feruloylated arabinoxylans with β -casein. *Journal of agricultural and food chemistry*, 52(21), 6633–6639.
- [24] Oudgenoeg, G., Dirksen, E., Ingemann, S., Hilhorst, R., Gruppen, H., Boeriu, C. G., ... & Voragen, A. G. (2002). Horseradish peroxidase-catalyzed oligomerization of ferulic acid on a template of a tyrosine-containing tripeptide. *Journal of Biological chemistry*, 277(24), 21332–21340.
- [25] Wozney, J. M., Rosen, V., Celeste, A. J., Mitsock, L. M., Whitters, M. J., Kriz, R. W., ... & Wang, E. A. (1988). Novel regulators of bone formation: molecular clones and activities. *Science*, 242(4885), 1528–1534.
- [26] Suzuki, Y., Tanihara, M., Suzuki, K., Saitou, A., Sufan, W., & Nishimura, Y. (2000). Alginate hydrogel linked with synthetic oligopeptide derived from BMP-2 allows ectopic osteoinduction in vivo. *Journal of biomedical materials research*, 50(3), 405–409.
- [27] Spicer, P. P., Kretlow, J. D., Young, S., Jansen, J. A., Kasper, F. K., & Mikos, A. G. (2012). Evaluation of bone regeneration using the rat critical size calvarial defect. *Nature protocols*, 7(10), 1918–1929.
- [28] Choi, Y. J., Lee, J. Y., Park, J. H., Park, J. B., Suh, J. S., Choi, Y. S., ... & Park, Y. J. (2010). The identification of a heparin binding domain peptide from bone morphogenetic protein-4 and its role on osteogenesis. *Biomaterials*, 31(28), 7226–7238.

- [29] Choi, Y. S., Lee, J. Y., Suh, J. S., Lee, G., Chung, C. P., & Park, Y. J. (2013). The mineralization inducing peptide derived from dentin sialophosphoprotein for bone regeneration. *Journal of Biomedical Materials Research Part A*, 101(2), 590–598.
- [30] Park, S. Y., Kim, K. H., Koo, K. T., Lee, K. W., Lee, Y. M., Chung, C. P., & Seol, Y. J. (2011). The evaluation of the correlation between histomorphometric analysis and micro-computed tomography analysis in AdBMP-2 induced bone regeneration in rat calvarial defects. *Journal of periodontal & implant science*, 41(5), 218–226.
- [31] Madej, T., Lanczycki, C. J., Zhang, D., Thiessen, P. A., Geer, R. C., Marchler-Bauer, A., & Bryant, S. H. (2014). MMDB and VAST+: tracking structural similarities between macromolecular complexes. *Nucleic acids research*, 42(D1), D297–D303.
- [32] Cohen, F. E., Sternberg, M. J., & Taylor, W. R. (1980). Analysis and prediction of protein beta-sheet structures by a combinatorial approach. *Nature*, 285(5764), 378–382.
- [33] Leckie, F., Mattei, B., Capodicasa, C., Hemmings, A., Nuss, L., Aracri, B., ... & Cervone, F. (1999). The specificity of polygalacturonase-inhibiting protein (PGIP): a single amino acid substitution in the solvent-exposed β -strand/ β -turn region of the leucine-rich repeats (LRRs) confers a new recognition capability. *The EMBO Journal*, 18(9), 2352–2363.

- [34] Holmes, R. E. (1979). Bone regeneration within a coralline hydroxyapatite implant. *Plastic and reconstructive surgery*, 63(5), 626–633.
- [35] Laurencin, C. T., Attawia, M. A., Elgendy, H. E., & Herbert, K. M. (1996). Tissue engineered bone–regeneration using degradable polymers: the formation of mineralized matrices. *Bone*, 19(1), S93–S99.
- [36] Yu, T., Volponi, A. A., Babb, R., An, Z., & Sharpe, P. T. (2015). Chapter Eight–Stem Cells in Tooth Development, Growth, Repair, and Regeneration. *Current topics in developmental biology*, 115, 187–212.
- [37] Yamada, Y., Boo, J. S., Ozawa, R., Nagasaka, T., Okazaki, Y., Hata, K. I., & Ueda, M. (2003). Bone regeneration following injection of mesenchymal stem cells and fibrin glue with a biodegradable scaffold. *Journal of Cranio–Maxillofacial Surgery*, 31(1), 27–33.
- [38] Stanciu, G. A., Sandulescu, I., Savu, B., Stanciu, S. G., Paraskevopoulos, K. M., Chatzistavrou, X., ... & Koidis, P. (2007). Investigation of the hydroxyapatite growth on bioactive glass surface. *Journal of Biomedical & Pharmaceutical Engineering*, 1(1), 34–39.
- [39] Foit, L., Morgan, G. J., Kern, M. J., Steimer, L. R., von Hacht, A. A., Titchmarsh, J., ... & Bardwell, J. C. (2009). Optimizing protein stability in vivo. *Molecular cell*, 36(5), 861–871.
- [40] Struck, J., Morgenthaler, N. G., & Bergmann, A. (2005). Copeptin, a stable peptide derived from the vasopressin

precursor, is elevated in serum of sepsis patients.
Peptides, 26(12), 2500–2504.

국문요약(국문초록)

골재생효과에 대한 합성 펩타이드 함유 하이드로젤의 기능성 연구

조 범 수

서울대학교 대학원 치의과학과
치의재생생명공학전공

(지도교수 박 윤 정)

줄기세포를 탑재 가능한 다공성 지지체, 멤브레인과 같은 생체재료는 골 재생 영역에서 우수한 골재생능을 보여주고 있다. 그 중 주입형 하이드로젤 시스템의 경우 다재다능함, 변형 가능함 그리고 손상된 영역에 시술 시 절개가 불필요하다는 편리성으로 인하여 각광받고 있다. 또한 단백질, 펩타이드 그리고 유전물질과 같은 생리활성 물질을 하이드로젤에 탑재가 가능하고 골재생을 위한 약물의 방출을 조절가능하다. 이러한 생리활성물질의 효능이 좋음에도 불구하고 젤 내부에 탑재하기에는 물질적인 한계가 존재한다. 하이드로젤과 생리활성물질의 단순 복합체의 경우 급속적인 약물 방출 같은 이유로 약물 조절이 한계가 있다. 그러므로

이를 대체하기 위하여 생리활성인자와 하이드로젤과의 결합 방법을 고안할 필요가 있다.

단백질의 경우 하이드로젤과의 화학적 결합으로 인하여 약효의 변화를 불러올 수 있다. 생리활성 펩타이드의 경우 하이드로젤과의 화학적 결합은 새로운 대안이 될 수 있을 것으로 예측된다. Osteopontin의 콜라겐 결합 모티프(CBM)에서 유래된 합성 펩타이드의 경우 이전 연구에 의하면 골분화 유도 가능성을 지닌다고 알려져 있다. 콜라겐 결합 모티프 펩타이드(CBMP)의 경우 중간엽 줄기세포를 골분화 유도를 가능케 하여 하이드로젤과의 결합 후보물질로 선정하였다. 하이드로젤의 경우 폐놀을 지니고 있는데 이는 과산화수소와 겨자무과산화효소에 의하여 폐놀과 폐놀이 서로 화학적인 결합을 유도하여 이를 이용, 젤화를 유도하는 방식이다. CBMP의 경우 타이로신이 존재하여 폐놀을 지니고 있어 젤화 유도를 과산화수소와 겨자무과산화효소로 유도 시 하이드로젤과 결합을 시도하였으며 동시에 줄기세포 또한 같이 포함하여 복합체 형성을 시도하였다.

CBMP-하이드로젤 복합체 내에서 줄기세포의 생존을 확인하였다. 또한 CBMP-하이드로젤 복합체 내부에서 줄기세포의 골분화 유도를 골분화 인자 단백질의 발현 증가, 알칼리성 인산가수 분해효소 활성화도 증가, 그리고 EDS를 통한 칼슘의 축적을 통하여 확인하였다. 더 나아가 동물 수준의 연구에서 줄기세포가 탑재된 CBMP-하이드로젤의 복합체를 백서 두개골 결손모델을 통하여 결손부가 BMP-2-하이드로젤과 비견하게 재생이 된 것을 확인할 수 있었다. 이러한 결과를 통하여 CBMP가 결합된 하이드로젤은 줄기세포의 골분화를 유도하는 능력을 지니고 있으며 그리고 조직재생을 위한 줄기세포의 운반 수단으로 이용 가능성을 확인할 수 있었다.

주요어 : 골조직재생, 합성 펩타이드, 콜라겐 결합 모티프, 하이드로젤, 줄기세포

학 번 : 2013-23551